

---

Theses and Dissertations

---

2012

# Industrially relevant epoxy-acrylate hybrid resin photopolymerizations

Gbenga I. Ajiboye  
*University of Iowa*

Copyright 2012 Gbenga I. Ajiboye

This dissertation is available at Iowa Research Online: <http://ir.uiowa.edu/etd/3558>

---

## Recommended Citation

Ajiboye, Gbenga I. "Industrially relevant epoxy-acrylate hybrid resin photopolymerizations." MS (Master of Science) thesis, University of Iowa, 2012.  
<http://ir.uiowa.edu/etd/3558>.

---

Follow this and additional works at: <http://ir.uiowa.edu/etd>

 Part of the [Chemical Engineering Commons](#)

INDUSTRIALLY RELEVANT EPOXY-ACRYLATE HYBRID RESIN  
PHOTOPOLYMERIZATIONS

by

Gbenga I. Ajiboye

A thesis submitted in partial fulfillment of the  
requirements for Master of Science degree  
in Chemical and Biochemical Engineering  
in the Graduate College of  
The University of Iowa

December 2012

Thesis Supervisor: Associate Professor, Julie L.P. Jessop

Copyright by

GBENGA I. AJIBOYE

2012

All Rights Reserved

Graduate College  
The University of Iowa  
Iowa City, Iowa

CERTIFICATE OF APPROVAL

---

MASTER'S THESIS

---

This is to certify that the Master's thesis of

Gbenga I. Ajiboye

has been approved by the Examining Committee for the thesis requirement for the Master of Science degree in Chemical and Biochemical Engineering at the December 2012 graduation.

Thesis Committee:

\_\_\_\_\_  
Julie L.P Jessop, Thesis Supervisor

\_\_\_\_\_  
Tonya L. Peeples

\_\_\_\_\_  
Chris Coretsopoulos

To all the women in my life, my mother, my wife Kemi and beautiful daughter Amari

‘The Lord protects those residing outside their native land; he lifts up the fatherless and the widow, but he opposes the wicked’

Psalm 146:9 NET

When you stifle human potential due to your ignorance, it hurts us all.

Bill Clinton

## ACKNOWLEDGEMENTS

I will like to thank the University of Iowa for admitting me to pursue a PhD degree in chemical engineering. This admission came after I have successfully completed a master's degree in Prairie View A&M University. It might be surprising to the readers that this thesis is for another master's degree; I will give a summary of that. The credit for another master's degree instead of PhD goes to my major adviser, her energy and style of micro-management that takes away passion, believe and enthusiasm from a minority student in a less diverse environment. I have accounted for my 40 hours every week for three years, studying photopolymerization. The genuine support for success was overshadowed by accounting for forty hours instead of helping with laboratory concerns, working diligently with graduate student to navigate through urgent personal and professional concerns and acting as an adversary behind the graduate student instead of an advocate. Never the less my major adviser worked diligently with approving another masters degree without questioning her conscience.

This acknowledgement will defeat its purpose if I fail to thank all the students in the Iowa City Community School District (ICCS) starting from 3rd to 12<sup>th</sup> grade, that have participated in the MESA Tutoring under my leadership for three years. The program was a success and its impact is that the under-represented and disadvantaged youth in the Iowa City school district were motivated to pursue STEM related field in college. All the volunteers that showed up every week for the tutoring, the faculty member that supported the program; Dr. Tonya Peebles and Dr. Vincent Rodgers, and the administrators that made sure we had the pizza paid for, Natalie Potter, I say a big thanks to you all. This program is my signature achievement in Iowa City.

Lastly, I will thank National GEM Consortium for the financial award, National Organization of Black Chemist and Chemical Engineers (NOBBChE) for the opportunity to win first place award in a regional contest, and the engineering faculty for Luther H. Smith, Honorable Service Award. My wife for the moral support through difficult times, my mother for helping with the care of our little princess while I was in the lab, and lastly my little princess Amari, for the joy and hope she brings to the family.



## ABSTRACT

Photopolymerization of epoxy-acrylate hybrid resins takes advantages of inherent properties present in the free-radical and cationic reactions to reduce oxygen inhibition problems that plague free-radical reactions. Similarly, the combined reaction mechanisms reduce moisture sensitivity of the cationic reactions. Despite the advantages of epoxy-acrylate hybrid resins, problems persist that need to be addressed. For example, low conversion and polymerization rate of the epoxides are a problem, because the fast acrylate conversion prevents the epoxide from reaching high conversion. Controlling phase separation is challenging, since two moieties with different properties are reacting. The physical properties of the polymer will be impacted by the availability of different moieties. High shrinkage stress results from the acrylate moiety, causing buckling and cracking in film and coating applications.

The overall goal of this study is to use the fundamental knowledge of epoxy-acrylate hybrid resins to formulate industrially viable polymers. In order to achieve this goal, the study focuses on the following objectives: (I) determine the apparent activation energy of the hybrid monomer METHB, (II) increase epoxide conversion and polymerization rate of hybrid formulations, and (III) control physical properties in epoxy-acrylate hybrid resins. In order to increase the epoxide conversion and rate of polymerization, the sensitivity of epoxides to alcohol is used to facilitate the activated monomer (AM) mechanism and induce a covalent bond between the epoxide and acrylate polymers through the hydroxyl group. It is hypothesized that if the AM mechanism is facilitated, epoxide conversion will increase. As a result, the resins can be tailored to control phase separation and physical properties, and shrinkage stress can be reduced.

In pursuit of these objectives, the hybrid monomer METHB was polymerized at temperatures ranging from 30°C to 70°C to obtain apparent activation energy of 23.49 kJ/mol for acrylate and 57 kJ/mol for epoxide moieties. Then, hybrid systems pairing hydroxyl-containing acrylates with epoxides were formulated to promote the faster AM mechanism. Monomer composition was changed in the presence of hydroxyl-containing acrylate, and initiators were carefully selected in order to control phase separation. The conversion of acrylate and epoxide was monitored in real time by Raman spectroscopy. The physical and mechanical properties were monitored using dynamic mechanical analysis. Epoxide conversion and rate of polymerization in epoxide-acrylate hybrid monomer systems were shown to increase through the introduction of a hydroxyl group on the meth/acrylate monomer, taking advantage of the faster AM mechanism. In addition, this covalent bond linking the epoxide network to the meth/acrylate polymer chains resulted in little or no phase separation and a reduction of the  $T_g$  for the hybrid polymer compared to the neat epoxide.

Fundamental knowledge gained from this research will enable the use of epoxy-acrylate hybrid resins in variety of applications. For instance, shrinkage may be reduced in dental fillings, noise and vibration problems in aircraft and other machinery may be controlled, and photopolymerization cost could be reduced in thin film applications.

## TABLE OF CONTENTS

LIST OF TABLES .....	x
LIST OF FIGURES .....	xii
LIST OF SCHEMES.....	xiv
<b>CHAPTER 1. INTRODUCTION AND BACKGROUND .....</b>	<b>1</b>
Introduction.....	1
Background.....	3
Acrylates.....	4
Free-Radical Reactions .....	4
Inhibition by Oxygen .....	6
Shrinkage of Acrylates .....	7
Epoxides .....	9
Cationic Ring-Opening Reactions.....	9
Sensitivity to Moisture and Alcohols.....	10
Hybrid resins .....	12
Hybrid Resin Reactions.....	12
Low Conversion and Polymerization Rate of Epoxides.....	13
Kinetic Analysis .....	14
Phase Separation of Hybrid Resins.....	15
Physical and Mechanical Analysis.....	17
Objectives .....	18
Notes .....	20
<b>CHAPTER 2. KINETIC STUDY FOR PHOTOPOLYMERIZATION OF HYBRID MONOMER METHB USING RAMAN SPECTROSCOPY.....</b>	<b>26</b>
Introduction.....	26
Experimental.....	28
Materials.....	28
Methods .....	29
Kinetic Studies using Raman Spectroscopy.....	29
Results and Discussion .....	30
Kinetic Rate Expressions.....	32
Rate of Polymerization of Hybrid Monomer, METHB.....	32
Propagation Rate Constant of METHB.....	36
Conclusion.....	40
Notes .....	42
<b>CHAPTER 3. CONVERSION ENHANCEMENT AND PHYSICAL PROPERTY CONTROL IN EPOXIDE-ACRYLATE HYBRID PHOTOPOLYMERIZATIONS WITH HYDROXYL-CONTAINING ACRYLATES.....</b>	<b>44</b>
Introduction.....	44
Experimental.....	46
Materials.....	46
Methods .....	47
Kinetic Studies using Raman Spectroscopy.....	47
Physical Property Studies using Dynamic Mechanical Analysis.....	48

Results and Discussion .....	49
Free-Radical Photopolymerization of Epoxy-Acrylate Hybrid Formulations.....	49
Cationic Ring-Opening Photopolymerization of Epoxy-Acrylate Hybrid Formulations .....	53
Physical Properties of Epoxide-Acrylate Hybrid Photopolymers .....	56
Conclusions.....	59
Notes .....	60
CHAPTER 4. CONCLUSIONS AND RECOMMENDATIONS .....	62
APPENDIX A. METHOD FOR ESTIMATION OF $k_t$ .....	64
APPENDIX B. LITERATURE VALUES FOR ACTIVATION ENERGIES OF CATIONIC RING-OPENING OF EPOXIDES .....	68
APPENDIX C. REPRESENTATIVE REAL-TIME RAMAN DATA FOR ISOTHERMAL PHOTOPOLYMERIZATIONS OF METHB IN CHAPTER 2 .....	69
APPENDIX D. SHRINKAGE STRESS ANALYSIS.....	73
Notes .....	75
REFERENCES .....	76

## LIST OF TABLES

Table A1.	Estimation of $k_t$ from dark polymerization experiments .....	67
Table B1.	Literature values for activation energies of cationic ring-opening of epoxides .....	68

## LIST OF FIGURES

Figure 1.1:	Benzoyl radical, $\alpha$ -cleavage of photoinitiator dimethoxyphenylacetophenone (DMPA) .....	5
Figure 1.2:	Molecular structure of generalized acrylate and its corresponding polymer repeat unit .....	6
Figure 1.3:	Generalized molecular structure of iodonium (left) and sulfonium salts (right) where $MX_n^-$ denotes metal halide.....	6
Figure 1.4:	Molecular structure of generalized aliphatic epoxide monomer and its corresponding polymer repeat unit.....	10
Figure 1.5:	Epoxy-acrylate hybrid resins; hybrid monomer molecule (left) and hybrid mixture (right) .....	10
Figure 1.6:	Characteristic peaks in Raman spectrum of HEA-EEC showing epoxide reactive band at $790\text{ cm}^{-1}$ and acrylate carbon double bond reactive band at $1640\text{ cm}^{-1}$ .....	15
Figure 2.1:	Molecular structure of hybrid monomer METHB .....	28
Figure 2.2:	Acrylate C=C conversion for hybrid monomer METHB with 0.17wt% DMPA and an effective irradiance of $100\text{ mW/cm}^2$ .....	31
Figure 2.3:	Conversion of epoxide ring for hybrid monomer, METHB with 0.5 wt% DAI and an effective irradiance of $100\text{ mW/cm}^2$ .....	31
Figure 2.4:	Acrylate C=C rate of polymerization for hybrid monomer, METHB with 0.17wt% DMPA and an effective irradiance of $100\text{ mW/cm}^2$ .....	33
Figure 2.5:	Epoxide rate of polymerization for hybrid monomer, METHB with 0.5 wt% DAI and an effective irradiance of $100\text{ mW/cm}^2$ .....	33
Figure 2.6:	Arrhenius plot for the acrylate C=C in hybrid monomer, METHB with 0.17wt% DMPA and an effective irradiance of $100\text{ mW/cm}^2$ . $k_p$ (L/(mol·s)) was obtained from equation 2.10, by substituting for the respective variables.....	38
Figure 2.7:	Arrhenius plot for the ring-opening polymerization of epoxide in hybrid monomer METHB with 0.5 wt% DAI and an effective irradiance of $100\text{ mW/cm}^2$ . $k_p$ (L/(mol·s)) was obtained from equation 2.12, by substituting for the respective variables.....	38
Figure 2.8:	Arrhenius plot for the acrylate C=C in hybrid monomer, METHB with 0.17wt% DMPA and an effective irradiance of $100\text{ mW/cm}^2$ . The data point for $70^\circ\text{C}$ has been removed.....	40
Figure 3.1:	Molecular structures of monomers and photoinitiator used in this study .....	46

Figure 3.2:	Acrylate C=C conversion for hybrid formulations of EEC-EGMEA (on a wt% basis) with 0.5 wt% DAI at 30°C and with an effective irradiance of 100 mW/cm <sup>2</sup> .....	50
Figure 3.3:	Acrylate C=C conversion for hybrid formulations of EEC-HEA (on a wt% basis) with 0.5 wt% DAI at 30°C and with an effective irradiance of 100 mW/cm <sup>2</sup> .....	50
Figure 3.4:	Acrylate conversion versus monomer viscosity in hybrid formulation of EEC-HEA and EEC-EGMEA. Viscosity of monomer composition is estimated using Refutas equation .....	52
Figure 3.5:	Epoxide conversion versus monomer viscosity in hybrid formulation of EEC-HEA and EEC-EGMEA. Viscosity of monomer composition is estimated using Refutas equation .....	53
Figure 3.6:	Conversion of epoxide ring for hybrid formulations of EEC-EGMEA (on a wt% basis) with 0.5 wt% DAI at 30°C and with an effective irradiance of 100 mW/cm <sup>2</sup> .....	54
Figure 3.7:	Conversion of epoxide ring for hybrid formulations of EEC-HEA (on a wt% basis) with 0.5 wt% DAI at 30°C and with an effective irradiance of 100 mW/cm <sup>2</sup> .....	55
Figure 3.8:	Tan δ plots, obtained by DMA, of EEC-EGMEA polymers. Hybrid formulations were photopolymerized with 0.5wt% DAI and 0.017 wt% DMPA at 30°C for 15 min using an effective irradiance of 100 mW/cm <sup>2</sup> , and the resulting polymers were heat treated at 150°C for 2 hours.....	57
Figure 3.9:	Tan δ plots, obtained by DMA, of EEC-HEA polymers. Hybrid formulations were photopolymerized with 0.5wt% DAI at 30°C for 15 min using an effective irradiance of 100 mW/cm <sup>2</sup> , and the resulting polymers were heat treated at 150°C for 2 hours.....	58
Figure C1:	Real-time waterfall picture of METHB with 0.17 wt% DMPA with an effective irradiance of 100 mW/cm <sup>2</sup> at 30°C. ....	69
Figure C2:	Real-time waterfall picture of METHB with 0.5 wt% DAI with an effective irradiance of 100 mW/cm <sup>2</sup> at 30°C. ....	70
Figure C3:	Real-time waterfall picture of METHB with 0.5 wt% DAI and 0.17 wt% DMPA with an effective irradiance of 100 mW/cm <sup>2</sup> at 30°C. ....	70
Figure C4:	Real-time waterfall picture of METHB with 0.17 wt% DMPA with an effective irradiance of 100 mW/cm <sup>2</sup> at 70°C. ....	71
Figure C5:	Real-time waterfall picture of METHB with 0.5 wt% DAI with an effective irradiance of 100 mW/cm <sup>2</sup> at 70°C. ....	71
Figure C6:	Real-time waterfall picture of METHB with 0.5 wt% DAI and 0.17 wt% DMPA with an effective irradiance of 100 mW/cm <sup>2</sup> at 30°C. ....	72

Figure D1: Schematic of polymerization stress tester, used to monitor polymerization shrinkage.....74



## LIST OF SCHEMES

Scheme 1.1: Chain polymerization mechanism.....	4
Scheme 1.2: Oxygen inhibition in free-radical photopolymerization .....	7
Scheme 1.3: Shrinkage from polymerization of carbon-carbon double bonds with Van der Waals distance. <sup>32</sup> .....	8
Scheme 1.4: Moisture and alcohol sensitivity of epoxides.....	12

## CHAPTER 1

### INTRODUCTION AND BACKGROUND

#### Introduction

Photopolymerization uses light, instead of heat, to initiate reactions that convert monomer to polymer. This process has led to increased productivity, new capabilities for end users, cost effectiveness, and environmental friendliness.<sup>1</sup> Photopolymerization has many unique advantages over conventional thermal processes. Reactions can take place at low or room temperatures, which decreases energy demands and reduces thermal runaway hazards. Spatial and temporal control is easy to achieve, as light can be directed to locations of interest in the system and is easily shuttered, which for certain formulations, allows one to start and stop the reaction as needed. Photopolymerizable monomers generally have very high rates of reaction, which allows for higher production speeds. Also, formulations are typically solvent-free, which reduce the emissions of volatile organic pollutants in comparison to thermal methods.<sup>2,3</sup>

Ultra-violet (UV) formulated product usage has experienced growth for 35 consecutive years, growing from 5,000 to 95,000 metric tons starting from 1970 to 2005. Many industries have benefited from the application of photopolymerization such as the coating, ink, and adhesive industries. Its application has also expanded into uses such as food packaging, interior and exterior design, and biomedical implants.<sup>4,5</sup>

In this study, the monomers in consideration are acrylates and epoxides, which undergo free-radical and cationic polymerization respectively. Acrylates have high reaction rates compared to epoxides, are amenable to high-speed processes, and exhibit rapidly decreased reaction rates upon shuttering the illumination source, which makes

them suitable for spatial and temporal control. They can be easily modified to obtain desired chemical, mechanical and optical properties for various applications. Epoxides have excellent mechanical properties, low shrinkage, chemical and heat resistance, excellent adhesion, and low toxicity.<sup>6,7</sup>

The major disadvantage of the free-radical reaction mechanism is sensitivity to oxygen. In order to overcome inhibition by oxygen, several costly approaches have been taken such as using inert gases to blanket the system and waxes or shielding films to prevent oxygen from entering the system. Cationic reactions, although not inhibited by oxygen, still pose their own challenges, such as moisture and alcohol sensitivity and slow reaction rates in comparison to free-radical reactions.<sup>4,8-10</sup>

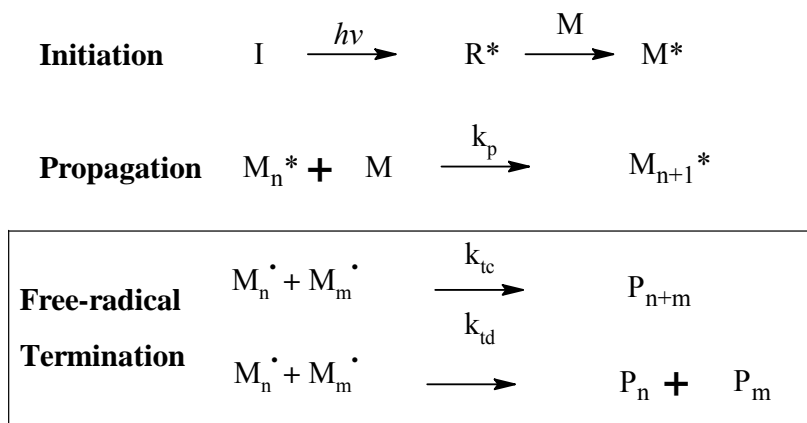
Researchers have attempted to address these drawbacks by developing hybrid systems that combine the two reaction mechanisms, free-radical and cationic, in order to take advantage of the unique properties inherent to each.<sup>11,12</sup> Hybrid photopolymerizations, which contain two functional groups polymerized by independent reaction mechanisms, have arisen in recent years. For example, free-radical and cationic photopolymerization systems like epoxide-acrylate<sup>12,13</sup> and acrylate-vinyl ether<sup>14,15</sup> hybrid systems have been reported. This study focuses on epoxide-acrylate hybrid systems, which have been shown to mitigate oxygen inhibition<sup>15,16</sup> and moisture problems<sup>17</sup> that plague free-radical and cationic polymerizations, respectively.

Despite the advantages of epoxy-acrylate hybrid resins, problems persist that need to be addressed. For example, low conversions and slow curing rates of epoxides is a problem, because the fast acrylate conversion prevents the epoxide from achieving high conversion. Phase separation is possible, since two moieties are reacting with different

properties; hence, controlling phase separation will add value to the hybrid resins. The physical properties of the polymer will be impacted by the availability of different moieties. Understanding ways of tailoring the properties of the hybrid resins is necessary in order to incorporate it in industrial applications. High shrinkage stress that results from the acrylate moiety lingers and will need to be reduced.<sup>2,18,19</sup>

### Background

The photopolymerization of acrylates and epoxides by free-radical and cationic reaction, respectively, are types of chain polymerizations. In chain polymerization, polymers are formed by the continuous addition of monomers to the growing chain one molecule at a time. It has three major kinetic steps: initiation, propagation, and termination. The initiation involves two steps: first, initiators are dissociated by light, to form reactive species ( $R^*$ ), and secondly, the reactive species reacts with a monomer ( $M$ ) to form a propagating chain ( $M^*$ ). All reactive species, whether initiator fragments or propagating chain ends are termed active centers. Propagation starts when the active center continues to add monomers to form a growing polymer chain ( $M_n^*$ ) as summarized in Scheme 1.1. The type of termination occurs depending on the reaction mechanism; for instance, in free-radical reaction, termination is either by combination or by disproportionation.<sup>4,10,20,21</sup>



Scheme 1.1: Chain polymerization mechanism

The acrylate and epoxide monomers have some inherent properties unique to each. Acrylate monomers are plagued by sensitivity to oxygen; they have faster reactions, and generally, they have lower transition temperature compared to the epoxide monomers. The epoxide monomers, on the other hand, are sensitive to moisture and alcohol, the reactions and conversions are slow, and epoxides in many instances have higher glass transition temperatures compared to acrylates. Some of these properties are desirable, while others are not; the study in Chapter 3 aims to enhance the desirable properties and minimize the undesirable properties of the polymer.<sup>22-24</sup>

### Acrylates

**Free-Radical Reactions:** In order to produce free radicals that initiate polymerization, photoinitiators decompose upon absorption of light to react with monomers as shown in Figure 1.1 Free-radical photoinitiators may be classified as unimolecular and bimolecular. With unimolecular photoinitiators, only one molecular species interacts with light to produce a free-radical active center. Most of these initiators are  $\alpha$ - or  $\beta$ -cleavable in a position relative to the carbonyl group; examples include benzyl

ketal, benzoin ether, and amino ketones. Bimolecular photoinitiators, on the other hand, require two molecular species to form the propagating radical: a photoinitiator that absorbs light and a co-initiator that serves as a hydrogen or electron donor, examples of bimolecular initiators are benzophenone derivatives and thioxathones.<sup>4,25</sup>

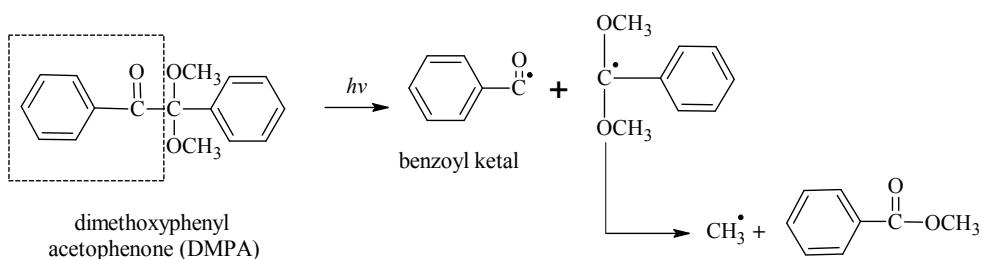
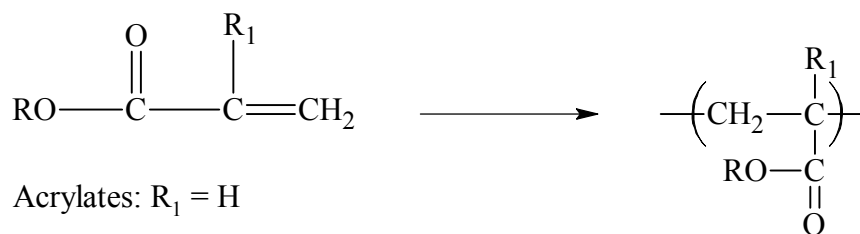


Figure 1.1: Benzoyl radical,  $\alpha$ -cleavage of photoinitiator dimethoxyphenylacetophenone (DMPA)

Monomers that accept a radical from an initiating species and then transfer that radical to another monomer to form a polymer are suitable for free-radical polymerization. Examples of monomers that satisfy this condition are acrylates, unsaturated ester/styrene, and olefins polyene monomers. The most widely used monomers for free-radical photopolymerization are acrylates and methacrylates. Figure 1.2 shows the generalized structure of the acrylate monomer and its corresponding polymer formed after reaction. These monomers, due to their high reaction rate, are amenable to high-speed processes desirable in many industries such as film and coating industries. They can be easily modified to obtain desired chemical, mechanical and optical properties for various applications. While polymerization of acrylates has many

advantages, the drawbacks include potential health hazards, volatility, unpleasant odor, oxygen inhibition and high shrinkage.<sup>2,26-28</sup>

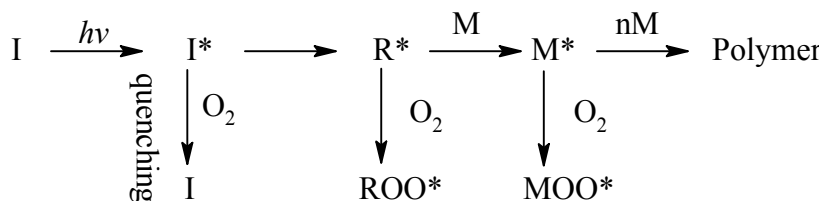


Acrylates:  $\text{R}_1 = \text{H}$

Methacrylates:  $\text{R}_1 = \text{CH}_3$

Figure 1.2: Molecular structure of generalized acrylate and its corresponding polymer repeat unit.

**Inhibition by Oxygen:** Molecular oxygen, which is present in air, inhibits free-radical photopolymerizations in several ways. It can react with the excited-state photoinitiator to quench the initiation reaction. Similarly, it can react with free radicals produced from photolysis ( $\text{R}^\bullet$ ) and propagating species ( $\text{M}_n^\bullet$ ) to form peroxy radicals, which are non-reactive towards acrylate double bonds. These inhibition mechanisms are shown in Scheme 1.2.<sup>16,24,29</sup> Thus, oxygen is an active chain terminator, which reduces the rate of polymerization in free-radical reactions. This limitation of free-radical polymerization has led to the exploration of other reaction mechanisms, such as the cationic polymerization of epoxides.



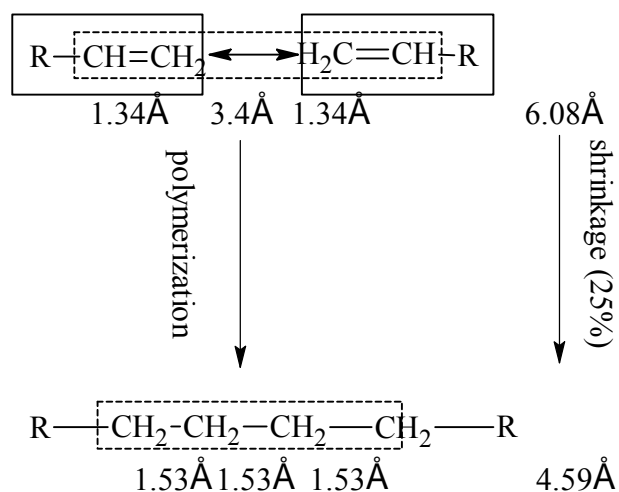
Scheme 1.2: Oxygen inhibition in free-radical photopolymerization

**Shrinkage of Acrylates:** Shrinkage is the volumetric decrease of the polymer unit until the reaction is terminated. It is an inherent phenomenon of polymers from the polymerization of carbon-carbon double bond monomers. The process occurs by the replacement of relatively weak, long-distance, intermolecular Van der Waals bonds by stronger, shorter, covalent bonds between the carbon atoms of different monomer units as shown in Scheme 1.3. Polymerization shrinkage is not a problem encountered in ring-opening polymerization such as epoxides where expansion rather than shrinkage can occur.<sup>30-32</sup>

Polymerization shrinkage is important to reduce because its adverse effects on the resulting polymer. For instance, in the case of coatings, the resulting tensile stress due to shrinkage may lead to cracking and delamination, posing a major problem to such applications.<sup>28</sup> In dental fillings, shrinkage increases failure during the functioning of the tooth. Introduction of inorganic non-shrinking phase to the polymer matrix is an approach that has been used to reduce shrinkage. However, this introduction has led to an increase in the stiffness of the material that is not desirable since cohesive fractures due to internal stresses can occur either in the tooth or in the composite.<sup>28,33-36</sup> Structural illumination, where a patterned light is chosen specifically for selected monomer or initiators polymerization, is used to reduce shrinkage stress. This method takes advantage of the



region in which different initiator absorbs light and the temporal ability of photopolymerization to set up the reaction sequence.<sup>37</sup> Other methods such as spiro-orthocarbonates, spiro-orthoesters, and other strained bicyclic monomers have been incorporated into curable formulations to reduce shrinkage.<sup>30,38</sup> Ethoxylated monomers, reaction temperature and speed, light intensity, and reversible addition fragmentation chain transfer have been reported to result in reduced polymerization shrinkage.<sup>28,39</sup> In Chapter 3, epoxides are mixed with acrylate resins and the reaction pattern sequenced without a structural illumination technique with an ultimate goal to reduce polymerization shrinkage. If successful, sample preparation and polymerization will be simpler with the new approach suggested by this study.



Scheme 1.3: Shrinkage from polymerization of carbon-carbon double bonds with Van der Waals distance.<sup>32</sup>

## Epoxides

**Cationic Ring-Opening reactions:** Cationic photoinitiators include the highly effective commercial iodonium and sulfonium salts, shown in Figure 1..<sup>40</sup> Upon photolysis, these salts undergo a homolytic cleavage to form an aryl cationic free radical and anion. The aryl free-radical cation abstracts hydrogen from a suitable hydrogen donor (R-H) to form an aryl acid. The dissociated anion recombines with the aryl acid to form a Bronsted acid. The Bronsted acid formed from the photolysis protonates the monomer, such as the epoxide as shown in Figure 1.4, to result in polymerization.<sup>20,41-43</sup>

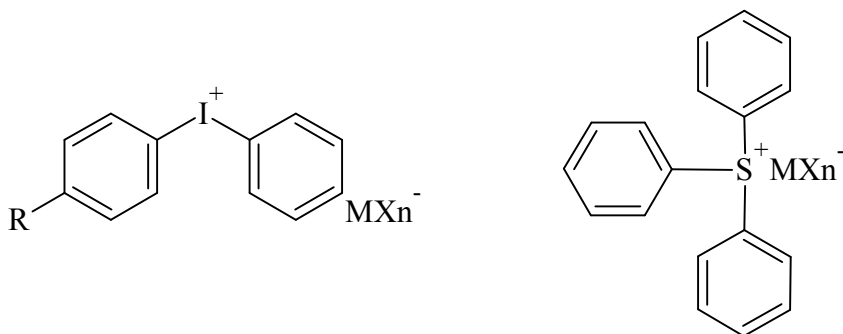


Figure 1.3: Generalized molecular structure of iodonium (left) and sulfonium salts (right) where MXn<sup>-</sup> denotes metal halide.

Various classes of monomers will undergo cationic chain polymerization, including epoxides, vinyl ethers, propenyl ethers, siloxanes, oxetanes, cyclic acetals, and furfural. The attributes of these polymers include excellent mechanical properties, low shrinkage, chemical and heat resistance, excellent adhesion, and low toxicity, making them important for a variety of commercial applications. Cationic polymerization has several advantages over free-radical polymerization: it is not inhibited by oxygen and has

long-lived active centers.<sup>20</sup> Despite the advantages of cationic reactions over free-radical reactions, cationic photopolymerizations based on epoxides have their drawbacks. They exhibit low conversion and reaction rates, have a narrow choice of efficient photoinitiators, and are sensitive to moisture and alcohol.<sup>44</sup>

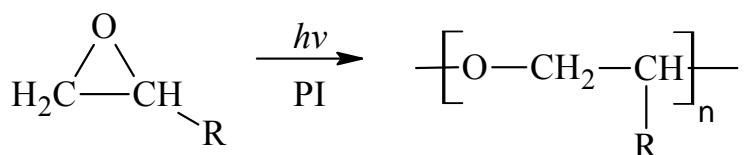


Figure 1.4: Molecular structure of generalized aliphatic epoxide monomer and its corresponding polymer repeat unit

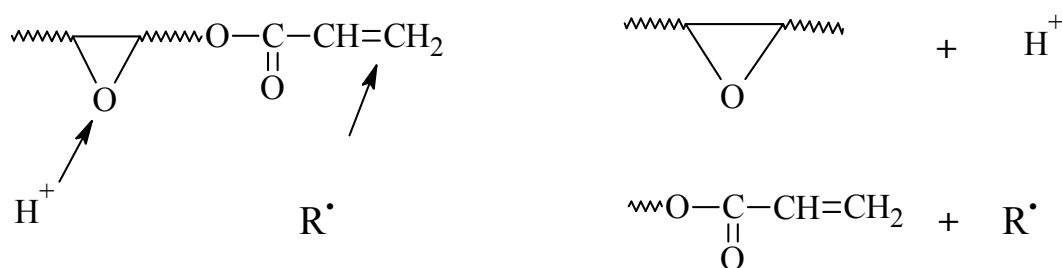


Figure 1.5: Epoxy-acrylate hybrid resins; hybrid monomer molecule (left) and hybrid mixture (right)

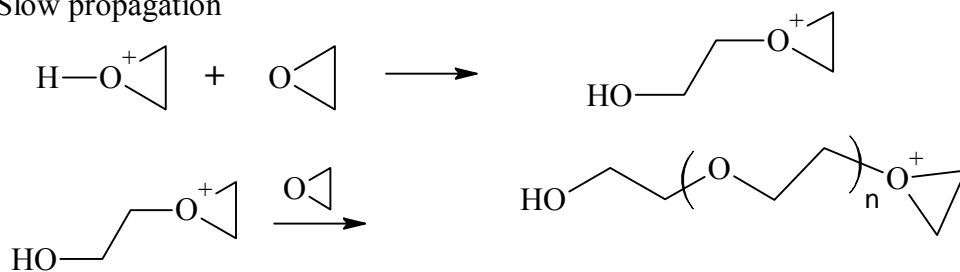
**Sensitivity to Moisture and Alcohols:** Water, which is often present as vapor in the atmosphere, has been shown to affect cationic polymerization in several ways. It can act as the hydrogen source to induce decomposition of the photoinitiator since an excessive amount of water can neutralize the initiator and inhibit the reaction through hydrolysis of the organic cation and anion of the super acid. Similarly, it can also participate in chain transfer reactions and consequently impact the final polymer properties.<sup>45,46</sup> Small amounts of water have been shown to reduce the average molecular

weight of linear polymer and the hardness of cross-linked polymers.<sup>47</sup> Propagation of the cationically polymerizable monomers, such as epoxides, proceeds through the active chain end (ACE) mechanism, shown in Scheme 1.4a.<sup>48</sup>

The presence of a nucleophilic species in the system, such as an alcohol, will result in a secondary reaction pathway: the activated monomer (AM) mechanism, shown in Scheme 1.4b. In this chain transfer reaction, a proton is exchanged rapidly between proton donors present in the system to activate other monomer molecules. The AM mechanism has been demonstrated to limit the chain length of the cured polymer, which has a pronounced effect on the mechanical properties of thin films.<sup>46</sup> The problem of the AM mechanism where the chain lengths are limited is addressed in Chapter 3, by incorporation of hydroxyl-containing acrylate monomer to form hybrid resins. The resulting reaction also covalently bonds the epoxide network to the acrylate chain through the hydroxides contained in the acrylate thereby reducing phase separation and lowering  $T_g$  of the polymer compared to the neat epoxide polymer.

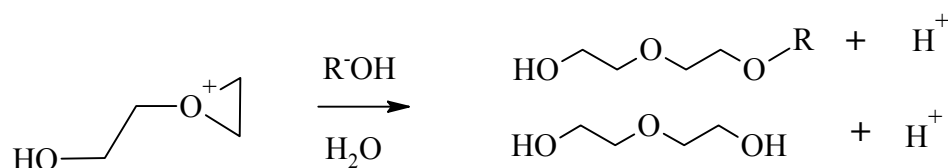
a : Active Chain End (ACE) mechanism

Slow propagation



b : Activated Monomer (AM) mechanism

Fast chain transfer



Scheme 1.4: Moisture and alcohol sensitivity of epoxides

### Hybrid Resins

**Hybrid Resin Reactions:** Hybrid resins combine two kinds of monomer functionalities to improve the reaction rate of the system and/or the physical properties of the polymer formed. Examples of hybrid systems include acrylate-epoxide, acrylate-alkyl and glycidyl, acrylate-oxetane systems, etc.<sup>8</sup> A hybrid monomer molecule is a single monomer with two functional groups, while a hybrid mixture is the combination of two monomers, each of different functional groups as shown in Figure 1.5. Hybrid resins of acrylate and epoxide moieties undergo simultaneous free-radical and cationic ring-opening polymerizations respectively. In the presence of a multi-functional monomer, the hybrid reaction can result in the formation of networks. Network formation in hybrid resins promise versatility in physical properties, because tuning of the polymer networks

is possible through chemical composition.<sup>13</sup> The combination of epoxides and acrylates monomers has been shown to reduce atmospheric sensitivity as compared to the neat formulations.<sup>2</sup> In recent studies by Cai et al., the presence of the acrylate moiety has resulted in reduced water and alcohol sensitivity of the cationic polymerization. Similarly, the epoxide moiety has been reported to provide an alternate reaction route at the surface where oxygen inhibition of acrylate is high, thereby reducing the inhibition effect.<sup>8,23,37,47</sup>

**Low Conversion and Polymerization Rate of Epoxides:** Cationic photopolymerization of epoxide has many advantages that are desirable in the hybrid polymers. It has led to reduced oxygen inhibition of the acrylate when hybrid acrylate/biscycloaliphatic epoxy are photopolymerized,<sup>49</sup> and lower shrinkage for dental application when methacrylate/vinyl ether hybrid systems were paired.<sup>15</sup> However, the limitation of low reaction rate and conversion persist in hybrid polymerization of epoxy-acrylate resins. For instance, although He et al. prepared a novel benzoyl-substituted diaryliodonium salt used for hybrid polymerization of cyclohexene oxide and methyl methacrylates, the result showed a lower epoxide conversion compared to the acrylate.<sup>50</sup> The much faster acrylate reaction interferes with epoxide conversion because the epoxide chain growth takes place via the relatively slow active chain end (ACE) mechanism.<sup>48</sup>

In an attempt to increase the epoxide conversion, hybrid monomers have been used in place of hybrid formulation. For instance, Yong et al. used a synthesized epoxy-acrylate hybrid monomer, epoxy-acrylate (EA) and epoxide-acrylate hybrid (EAH), to obtain increased epoxide conversion.<sup>23</sup> Cai et al., when considering the effect of water concentration on a commercially available hybrid monomer, 3,4-epoxy-cyclohexyl-

methyl methacrylate, (METHB), obtained promising results that showed an improved epoxide conversion.<sup>47</sup> Crivello et al. combined multi-functional glycidyl ethers and 3,3-disubstituted oxetane into acrylate monomers to accelerate the epoxide conversion.<sup>8</sup>

The aim of the study in Chapter 3 is to use commercially available monomers to increase epoxide conversion, with simpler sample preparation. The AM mechanism will be facilitated by pairing a hydroxyl-containing acrylate with epoxide. It is expected that this pairing in the presence of free-radical and cationic initiators will result in the covalent bonding of the epoxide network to the acrylate chain through the hydroxides contained in the acrylate, thereby reducing phase separation and lowering  $T_g$  of the polymer compared to the neat epoxide polymer.

**Kinetic Analysis:** Raman spectroscopy is used to monitor the polymerization rate and conversion of epoxide and acrylate moieties. Raman spectroscopy is based on light scattering principles. It has been widely applied to structural studies of polymers because it can identify the chemical structure by detecting the rotational and vibrational transition in molecules and can follow the change of chemical bonds during polymerization.<sup>51</sup> Raman spectroscopy is not limited to kinetics analysis, but has been applied in several ways, including to characterize polymers,<sup>51</sup> for cure monitoring,<sup>52</sup> to demonstrate oxygen inhibition,<sup>2</sup> and to study polymers and polymerization process.<sup>53</sup>

Raman scattering occurs on the picoseconds time scale, enabling monitoring of rapid reactions in real time. In addition, the method requires minimal sample preparation, and variety of samples can be analyzed.<sup>54-56</sup>

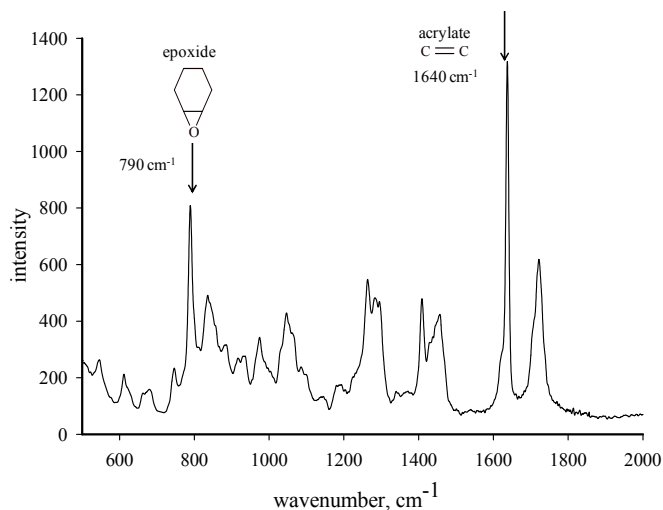


Figure 1.6: Characteristic peaks in Raman spectrum of HEA-EEC showing epoxide reactive band at 790 cm<sup>-1</sup> and acrylate carbon double bond reactive band at 1640cm<sup>-1</sup>

The Raman spectrum of hybrid formulation of HEA-EEC is shown in Figure 1.6. The epoxide reactive peak is at 790 cm<sup>-1</sup>, while the acrylate reactive peak is at 1640 cm<sup>-1</sup>. If spectral baselines remain constant through the reaction, Raman spectra are converted to conversion ( $\alpha$ ) by ratioing the peak area of reactive Raman bands before and during reaction ( $A_{rxn}(0)$  and  $A_{rxn}(t)$ , respectively) according to Equation 1.1.<sup>57</sup>

$$\alpha = 1 - \frac{A_{rxn}(t)}{A_{rxn}(0)} \quad (1.1)$$

**Phase Separation of Hybrid Resins:** Phase separation is a phenomenon that occurs when mixture of two or more monomer moieties separate into distinct regions (or phases) with different chemical composition and physical properties.<sup>58</sup> The domain size of each moiety may increase because of hydrodynamic flow and diffusion of the monomer mixture. The different domains can be grouped into two, in terms of the composition symmetry: a droplet pattern for an asymmetric mixture and a bi-continuous



pattern for a symmetric mixture. In a dynamic asymmetric mixture, the diffusion of the fast dynamic phase is prevented by the slow dynamic phase, thereby retarding the reaction of the fast dynamic phase by the slow dynamic phase. If the viscosity of the mixture is low, the reaction of the fast dynamic phase is fast, and polymer is formed; diffusion of the dynamic phase will prevent equilibrium, and in this case, a double phase is present.<sup>58-60</sup> Phase separation commonly occurs during curing processes due to the thermodynamic incompatibility between the components<sup>61,62</sup> and/or different kinetics exhibited by the moieties present.<sup>63</sup>

In a recent study, silicon resins carrying Si-H, Si-CH=CH<sub>2</sub> and Si-OH groups were blended with diglycidyl ether of hydrogenated bisphenol A (DGEHBA) to control phase separation<sup>18</sup> for an optically clear silicone/epoxy polymer. In the study, the composition of the monomer blend was important in the curing kinetics and controlling phase separation: when Si-OH reacted with the epoxy resins, phase separation was prevented. Phase separation has also been studied and controlled in polymerization of hybrid compositions based on urethane-acrylates,<sup>64</sup> alkylid-epoxide resins, and polyisocyanates<sup>61</sup> because they contain compounds that cure by different mechanisms. Phase separation can be determined by different analytical methods. In some instances, these methods are combined with differential scanning calorimetric (DSC), scanning electron microscopy (SEM), or dynamic mechanical analysis (DMA).<sup>18,64</sup> The presence or absence of double peaks in tan delta traces from DMA or heat flow traces from DSC is an indication of the presence or absence of microscopic phase separation in the polymer materials.

In Chapter 3, epoxy-acrylate hybrid mixtures were polymerized to control phase separation. Formulation composition, initiator choice, and reaction kinetics were used to control phase separation.

**Physical and Mechanical Analysis:** Dynamic mechanical analysis (DMA) can be used to analyze material response when an oscillating force is applied to a sample as a function of temperature and time. Several properties can be calculated from the material response, such as tendency to flow (viscosity) from the phase lag and the stiffness (modulus) from the sample recovery,  $\tan \delta$ , and glass transition temperature ( $T_g$ ).<sup>65</sup> DMA is the most preferred technique for measuring  $T_g$ , followed by differential scanning calorimetry (DSC). Other measuring techniques are available, but are less sensitive, such as thermo-mechanical analysis (TMA) and dielectric thermal analysis (DEA).<sup>22</sup>

In a DSC,  $T_g$  is denoted as the point of inflection in the step change observed in the heat flow curve for a small amount of material.<sup>66</sup> The concern is that the small amount of material may not be representative of the overall polymer. In a TMA,  $T_g$  is defined as the onset change in rate of expansion from either side of the step transition during temperature ramping of the dimensional changes in material as a function of temperature, time, and applied force. These measurements can be operator dependent and may result in inconsistent reporting of the transition temperature.<sup>67</sup>

The results from DMA have been used to classify other inherent properties of polymers, including determination of network properties of thiol-ene/acrylate systems,<sup>68</sup> characterization the viscoelastic properties of denture base resins with different curing modes,<sup>69</sup> and classification of polymer glass transition temperature and microscopic

phase separation.<sup>23,68</sup> In Chapter 3, DMA was used to determine  $T_g$ , modulus, and microscopic phase separation of hybrid resins.

### Objectives

The overall goal of this study is to use the fundamental knowledge of epoxy-acrylate hybrid resins to formulate industrially viable polymers. In order to achieve this goal, the study focuses on the following objectives: (I) investigate the kinetics and apparent activation energy of the hybrid monomer METHB, (II) increase epoxide conversion and polymerization rate of hybrid formulation, and (III) control physical properties in epoxy-acrylate hybrid resins. In order to increase the epoxide conversion and rate of polymerization, the sensitivity of epoxides to alcohol is used to facilitate the activated monomer (AM) mechanism and induce a covalent bond between the epoxide and acrylate polymers through the hydroxyl group. It is hypothesized that if the AM mechanism is facilitated, epoxide conversion will increase. As a result, the resins can be tailored to control phase separation and physical properties, and shrinkage stress can be reduced.

In Chapter 2, the hybrid monomer METHB was polymerized at temperatures ranging from 30°C to 70°C to obtain the apparent activation energy for the acrylate and epoxide moieties. In Chapter 3, hydroxyl-containing acrylates were paired with epoxides to promote the faster AM mechanism. The conversion of acrylate and epoxide was monitored in real time by Raman spectroscopy. Monomer composition was changed in the presence of hydroxyl-containing acrylate, and initiators were carefully selected in order to control phase separation. The high glass transition temperatures of the epoxide monomer were used to influence thermal and mechanical properties such as toughness,

stress at break, and high temperature creep resistance while retaining ease of processability provided by the acrylate monomer. The physical and mechanical properties were monitored using DMA.

Fundamental knowledge gained from this research will enable the use of epoxy-acrylate hybrid resins in variety of applications. For instance, shrinkage may be reduced in dental fillings, noise and vibration problems in aircraft and other machinery may be controlled, and photopolymerization cost could be reduced in thin film applications.

### Notes

1. Fouassier, J.P. Photopolymerization Reactions Under Visible Lights: Principle, Mechanisms and Examples of Applications. *Progress in Organic Coatings*. 2003;47:16-36.
2. Cai, Y.; Jessop, J.L.P. Decreased Oxygen Inhibition in Photopolymerized Acrylate/Epoxide Hybrid Polymer Coatings as Demonstrated by Raman Spectroscopy. *Polymer*. 2006;47:6560-6566.
3. Gleeson, M. Modeling the Photochemical Effects Present during Holographic Grating Formation in Photopolymer Materials. *Journal of Applied Physics*. 2007;102(2); 023108-1-023108-8
4. Cai, Y.; Jessop, J.L.P. Photopolymerization, Free Radical. In *Encyclopedia of Polymer Science and Technology*. 2003:807-837.
5. Gary, C. RadTech Annual Review, 2005-2006.  
[http://www.radtech.org/corporate/press2006/RT\\_Annual\\_Report\\_05-06.pdf](http://www.radtech.org/corporate/press2006/RT_Annual_Report_05-06.pdf).  
(Accessed June, 12th, 2010).
6. Braslau, R. Handbook of Radical Polymerization. Edited by Krzysztof Matyjaszewski, (Carnegie Mellon University) and Thomas P. Davis, (University of New South Wales). John Wiley & Sons, Inc.: Hoboken. *Journal of American Chemical Society*. 2003;125:3399-3400.
7. Cho, J. UV-initiated Free-radical and Cationic Photopolymerizations of Acrylate/Epoxide and Acrylate/Vinyl Ether Hybrid Systems with and without Photosensitizer. *J Applied Polymer Science*. 2004;93:1473.
8. Crivello, J. Synergistic Effects in Hybrid Free Radical/Cationic Photopolymerizations. *Journal of Polymer Science. Part A, Polymer Chemistry*. 2007;45:3759.
9. O'Brien, K.A.; Bowman, C.N. Modeling the Effect of Oxygen on Photopolymerization Kinetics. *Macromolecular Theory and Simulations*. 2006;15:176-182.
10. Benson, S.W.; North, A.M. The Kinetics of Free Radical Polymerization under Conditions of Diffusion-Controlled Termination. *Journal American Chemical Society*. 1962;84:935-940.
11. Strehmel, V.; Strehmel, B. Photoinduced Crosslinking of a Liquid-Crystalline Monomer in Thin Films. *Thin Solid Films*. 1996;284:317.
12. Oxman, J.D.; Jacobs, D.W.; Trom, M.C.; Sipani, V.; Ficek, B.; Scranton, A.B. Evaluation of Initiator Systems for Controlled and Sequentially Curable Free-

- radical/Cationic Hybrid Photopolymerizations. *Journal of Polymer Science Part A: Polymer Chemistry*. 2005;43:1747-1756.
13. Decker C. UV-radiation curing of acrylate/epoxide systems. *Polymer*. 2001;42:5531-5541.
  14. Rajaraman, S.K.; Mowers, W.A.; Crivello, J.V. Interaction of Epoxy and Vinyl Ethers during Photoinitiated Cationic Polymerization. *J Polymer Science Part A*. 1999;37:4007-4018.
  15. Lin, Y.; Stansbury, J.W. Kinetics Studies of Hybrid Structure Formation by Controlled Photopolymerization. *Polymer*. 2003;44:4781-4789.
  16. Studer, K.; Decker, C.; Schwalm, R. Overcoming Oxygen Inhibition in UV-curing of Acrylate Coatings by Carbon dioxide Inerting: Part II. *Progress in Organic Coatings*. 2003;48:101-111.
  17. Crivello, J.V. Photoinitiated Cationic Photopolymerization. *Annual review of materials science*. 1983;13:173-190.
  18. Zhang, Y.; Yang, X.; Zhao, X.; Huang, A. Synthesis and Properties of Optically Clear Silicone Resin/Epoxy Resin Hybrids. *Polymer International*. 2012;61:294-300.
  19. Decker, C. Photoinitiated Crosslinking Polymerization. *Progress in Polymer Science*. 1996;21:593-650.
  20. Sipani, V.; Scranton, A.B. Photopolymerization, Cationic. In *Encyclopedia of Polymer Science and Technology*. 2003:784-807.
  21. Andrzejewska, E. Photopolymerization Kinetics of Multifunctional Monomers. *Progress in polymer science*. 2001;26:605-665.
  22. Foreman, J. Dynamic Mechanical Analysis of Polymers. *American Laboratory*. 1997;29:21-24.
  23. He, Y. Photopolymerization Kinetics of Cycloaliphatic Epoxide-Acrylate Hybrid Monomer. *Polymer International*. 2007;56:1292-1297.
  24. Hofer, M.; Moszner, N.; Liska, R. Oxygen Scavengers and Sensitizers for Reduced Oxygen Inhibition in Radical Photopolymerization. *Journal Polymer Science Part A*. 2008;46:6916-6927.
  25. Monroe, B. Photoinitiators for Free-Radical-Initiated Photoimaging Systems. *Chemical Review American Chemical Society*. 1993;93:435-448.
  26. Wight, F. Oxygen Inhibition of Acrylic Photopolymerization. *Journal of Polymer Science Polymer Letter Edition* 1978;16:121-127.

27. Yamada, B.; Kobatake, S.; Aoki, S. Rate Constants for Elementary Reactions of the Radical Polymerization of Methyl 2-(Benzyloxymethyl)Acrylate as Polymerizable Acrylate Bearing Large Substituents. *Macromolecular Chemistry and Physics*. 1994;195:933-942.
28. Sartomer Application Bulletin. Shrinkage of UV Monomers. <http://www.sartomer.com/TechLit/4029.pdf>. 2011 (Accessed, Feb, 1st 2012).
29. Chong, J.S. Oxygen Consumption During Induction Period of Photopolymerizing System. *Journal of Applied Polymer Science*. 1969;13:241.
30. Williams, J.B.; Takeshi, E.; Radical Ring-Opening Polymerization and Copolymerization with Expansion in Volume. *Journal of Polymer Science, Polymer Symposia*. 1978;64:17-26.
31. Leung, D.; Bowman, C.N. Reducing Shrinkage Stress of Dimethacrylate Networks by Reversible Addition-Fragmentation Chain Transfer. *Macromolecular chemistry and Physics*. 2012;213:198-204.
32. Keogh, T.P. Vacuum or Suction Adhesion. <http://www.blogdental.es/Keogh/?p=131>. (Accessed, March 8th, 2012).
33. Geiser, V. Conversion and Shrinkage Analysis of Acrylated Hyperbranched Polymer Nanocomposites. *Journal of applied polymer science*. 2009;114:1954-1963.
34. Davidson, C.L.; Feilzer, A.J. Polymerization Shrinkage and Polymerization Shrinkage Stress in Polymer-Based Restoratives. *Journal Dental Research*. 1997;25:435-440.
35. Sartomer Application Bulletin. UV Curable Monomers Properties: Shrinkage and Glass Transition. <http://www.sartomer.com/TechLit/4039.pdf>. 2011. (Accessed, Feb, 1st 2012).
36. Dewaele, M. Volume Contraction in Photocured Dental Resins: The Shrinkage-Conversion Relationship Revisited. *Dental Materials*. 2006;22:359-365.
37. Peter, D.G. Structured Illumination as a Processing Method for Controlling Photopolymerized Coating Characteristics. *PhD Thesis, University of Iowa*, 2007.
38. Sangermano, M.; Carbonaro, W.; Malucelli, G.; Priola, A. Bicyclo-Orthoester as a Low-Shrinkage Additive in Cationic UV curing. *Polymer International*. 2007;56:1224-1229.
39. Rhodes K. Adhesives Deliver Low Shrink, Low Stress Bonds and Fast UV Cure. *Proceedings of SPIE--the international society for optical engineering*. 2001;4253:92-107.

40. Koleske, J.V. Cationic Photoinitiators and Initiation Mechanism. *In Radiation Curing of Coatings, ASTM International. Bridgeport, NJ. 2002:55-67.*
41. Abdul-Rasoul, F.A.M. Photochemical and Thermal Cationic Polymerizations Promoted by Free Radical Initiators. *Polymer. 1978;19:1219.*
42. Schikowsky, V.; Timpe, H. Investigation on Photolysis of Diaryliodonium Salts. *Journal für Praktische Chemie. 1989;331:447-460.*
43. Jančovičová, V.; Brezová, V.; Ciganek, M.; Cibulková, Z. Photolysis of Diaryliodonium Salts (UV/Vis, EPR and GC/MS investigations). *Journal Photochemistry and Photobiology A. 2000;136:195-202.*
44. Crivello J. Design and Synthesis of Highly Reactive Photopolymerizable Epoxy Monomers. *Journal of Polymer Science. Part A, Polymer chemistry. 2001;39:2385-2395.*
45. Palmese, G.R.; Ghosh, N.N.; McKnight, S.H. Investigation of Factors Influencing the Cationic Polymerization of Epoxy Resins. *International SAMPE Symposium and Exhibition. 2000;45.*
46. Ghosh, N.; Palmese G. Electron-Beam Curing of Epoxy Resins: Effect of Alcohols on Cationic Polymerization. *Bulletine of Material Science. 2005;28:603-607.*
47. Cai, Y. Effect of Water Concentration on Photopolymerized Acrylate/Epoxy Hybrid Polymer Coatings as Demonstrated by Raman Spectroscopy. *Polymer. 2009;50:5406.*
48. Bednarek, M.; Kubisa, P.; Penczek, S. Coexistence of Activated Monomer and Active Chain End Mechanisms in Cationic Copolymerization of Tetrahydrofuran with Ethylene oxide. *Macromolecules. 1999;32:5257-5263.*
49. Decker, C.; Viet, T.N.T.; This, H.P. Photoinitiated Cationic Polymerization of Epoxides. *Polymer International. 2001;50:986-997.*
50. He, J.; Mendoza, V.S. Synthesis and Study of a Novel Hybrid UV Photoinitiator: p-benzoyldiphenyliodonium hexafluorophosphate ( $\text{PhCOPhI}^+ \text{PhPF}_6^-$ ). *Journal of polymer science. Part A, Polymer chemistry. 1996;34:2809-2816.*
51. Maddams W, Gerrard D. Polymer Characterization by Raman-Spectroscopy. *Applied spectroscopy reviews. 1986;22:251-334.*
52. Nelson, E.W.; Scranton, A.B. In Situ Raman Spectroscopy for Cure Monitoring of Cationic Photopolymerizations of Divinyl Ethers. *Journal of Raman Spectroscopy. 1996;27:137-137.*



53. Johnson, A.; Lewis, I.; Edwards, H. Applications of Raman-Spectroscopy to The Study of Polymers and Polymerization Process. *Journal of Raman Spectroscopy*. 1993;24:475-483.
54. Johnson, C.K. Picosecond Timescale Raman Processes and Spectroscopy. *Pure and applied chemistry*. 1984;57:195-200.
55. Maslyuk, A. F.; Khranovskii, V.A.; Lipatov, Y.S.; Grishchenko, V. K. IR-Spectroscopic Study of the Process of Photopolymerization of Polyvinyl Compounds. *Polymer science*. 1984;26:1479-1483.
56. Krzysztof, L. Spectroscopic and Photopolymerization Studies of Benzyl Methacrylate/Poly(Benzyl Methacrylate) Two-Component System. *Journal of polymer science.Part B, Polymer physics*. 2010;48:1336-1348.
57. Doorn, S. Raman Spectroscopy and Imaging of Ultralong Carbon Nanotubes. *The journal of physical chemistry. B*. 2005;109:3751-3758.
58. Tanaka, H. Coarsening Mechanisms of Droplet Spinodal Decomposition in Binary Fluid Mixtures. *Journal of Chemical Physics*. 1996;105:10099-10099.
59. Mathew, Viju.; Sinturel, C. Epoxy Resin/Liquid Natural Rubber System: Secondary Phase Separation and its Impact on Mechanical Properties. *Journal of Material Science*. 2010;45:1769-1781.
60. Sangermano, M.; Carbonaro, W.; Malucelli, G.; Priola, A. UV-Cured Interpenetrating Acrylic-Epoxy Polymer Networks: Preparation and Characterization. *Macromolecular Materials and Engineering*. 2008;293:515-520.
61. Gudzera, S.S. Microphase Structure of Photopolymerizable Hybrid Adhesives Based on Urethane-Acrylates, Alkyd-Epoxy Resins and Polyisocyanates. *Polymer Science Series A*. 1991;33:2288-2295.
62. Bates, F.S. Polymer-Polymer Phase Behavior. *Science*. 1991;251:898-905.
63. Mitlin, V.S.; Manevich, L.I. Kinetically Stable Structures in the Nonlinear Theory of Spinodal Decomposition. *Journal of polymer science.Part B, Polymer physics*. 1990;28:1-16.
64. Ju-Young, K.; Yong-Seok, C.; Kyung-DO, S. Microphase-Separated Structure of Telechelic Urethane Acrylate Anionomers and Their Network in Various Solvents. *Journal of polymer science.Part B, Polymer physics*. 2000;38:2081-2095.
65. Menard K. Dynamic Mechanical Analysis: A Practical Introduction. *Second Edition*. *CRC Press Boca Raton London New York Washington, D.C.* 2008.

66. Montserrat, S. Measuring the Glass Transition of Thermosets by Alternating Differential Scanning Calorimetry. *Journal of Thermal Analysis and Calorimetry*. 2000;59:289-303.
67. Khandare, P.M. Measurement of the Glass Transition Temperature of Mesophase Pitches using a Thermomechanical Device. *Carbon*. 1996;34:663-669.
68. Wei,H.; Senyurt, A.F.;Jonsson, S.E.;Hoyle, C.E. Photopolymerization of Ternary Thiol-Ene/Acrylate Systems: Film and Network Properties. *Journal of polymer science.Part A, Polymer chemistry*. 2007;45:822-829.
69. Vaidyanathan,J.; Vaidyanathan, T.K. Dynamic Mechanical Analysis of Heat, Microwave and Visible Light Cure Denture Base Resins. *Journal of Materials Science, Materials in Medicine*. 1995;6:670-674.

## CHAPTER 2

KINETIC STUDY FOR PHOTOPOLYMERIZATION OF  
HYBRID MONOMER METHB USING RAMAN  
SPECTROSCOPYIntroduction

Photopolymerization, because of its unique advantages, has become well-accepted in many industrial applications such as coating glass fibers,<sup>1</sup> textile printing, and sunlight curing of waterborne latex paints.<sup>2</sup> Reactions can occur at low or room temperature, thereby decreasing energy demand and reducing thermal runaway hazards. Spatial control is readily achieved, as light can be directed to the location of interest in the system and is easily shuttered. Likewise, temporal control is easily achievable in the acrylate as one can start and stop the reaction as needed.<sup>3</sup>

The use of hybrid photopolymerization, which contains two functional groups polymerized by different reaction mechanisms, has been increasing in recent years. Commonly reported are the free-radical and cationic polymerization systems such as thiol-ene vinyl ether,<sup>4</sup> methacrylate-vinyl ether,<sup>5</sup> and epoxy-acrylate<sup>6</sup> hybrid systems. The hybrid resins may consist of hybrid monomer, which combines two functional groups in a single monomer, or a hybrid mixture, in which the two functional groups are on separate molecules. The main attribute of hybrid photopolymerization is that it synergistically combines the advantages of the inherent properties of the reacting moieties in the reaction. For example, atmospheric sensitivity of the acrylate to oxygen can be reduced,<sup>7</sup> and the sensitivity of epoxides to moisture may be overcome in a hybrid reaction.<sup>8</sup>

The photopolymerization of epoxy-acrylate hybrid resins occur by independent cationic and free-radical reactions, respectively. The two reactions are a form of chain

polymerization in which polymers are formed by continuous addition of monomer to the growing chain, one molecule at a time. It consists of three major kinetic steps (as was shown in Scheme 1.1): initiation, propagation, and termination (applicable to the free-radical reactions as cationic reactions generally lead to a chain transfer reaction<sup>9</sup>).

Independent kinetic studies of free-radical<sup>10</sup> and cationic<sup>11-13</sup> reactions by differential scanning calorimetry (DSC) and other methods are readily available. Similarly, the kinetic studies of synthesized cycloaliphatic epoxide-acrylate hybrid monomer by real-time infrared (RTIR) spectroscopy have been reported.<sup>14</sup> The commercially available hybrid monomer METHB has been investigated by Raman spectroscopic and microscopic method for its decreased oxygen inhibition effect<sup>7</sup> and its lower sensitivity to water compared to traditional epoxide systems.<sup>15</sup> However, activation energy of the epoxy-acrylate hybrid monomer of METHB has not been reported.

Typical activation energy of propagation for methacrylate<sup>16</sup> is 22.36 kJ/mol as monitored by pulsed laser polymerization (PLP), and those for epoxides<sup>11-13</sup> are listed in Table B1 of Appendix B. It has been difficult to use any of the DSC, PLP or RTIR methods for kinetic study analysis of hybrid resins because of the presence of acrylate and epoxide moiety in a single monomer. The aim of this study is to determine the activation energy for the acrylate and epoxide moieties on the hybrid monomer METHB using Raman spectroscopy for future modeling studies.

Raman spectroscopy has the advantage of monitoring simultaneously the rate of photopolymerization and conversion of epoxide and methacrylate moieties in real-time. Using conversion profiles obtained from Raman spectra, propagation rate constant from experimental data,  $k_p$ , was empirically obtained, and the apparent activation energy (the

apparent activation energy may not be true activation energy, but is within the range of true activation energy due to other experimental variables), was calculated using the Arrhenius relationship.<sup>9</sup>

## Experimental

### Materials

The epoxide/methacrylate hybrid monomer 3,4-epoxy-cyclohexyl-methyl methacrylate (METHB, Diacel) (see Figure 2.1) was used in this study. 2,2-Dimethoxy-2-phenyl-acetophenone (DMPA, Aldrich) was used to initiate the free-radical (methacrylate) reaction, while diaryliodonium hexafluoroantimonate (DAI, Sartomer) was utilized to initiate the cationic (epoxide) ring opening reaction. All materials were used as received.

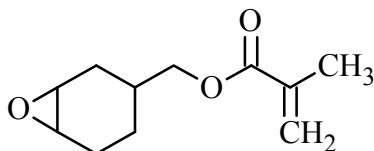


Figure 2.1: Molecular structure of hybrid monomer METHB

## Methods

### Kinetic Studies using Raman Spectroscopy

Raman spectroscopy was used to monitor the rate of photopolymerization and conversion of epoxide and methacrylate moieties in real-time. A 785-nm near-infrared laser was used to induce the Raman scattering effect. A Mark II holographic fiber-coupled stretch probehead (Kaiser Optical Systems, Inc.) attached to the HoloLab 5000R modular research Raman spectrograph was used to obtain spectra of the hybrid formulations during photopolymerization. The exposure time for each spectrum was 200 ms. Samples were isothermally cured at temperatures ranging from 30°C to 70°C in 1-mm ID quartz capillary tubes. The isothermal temperature was achieved by passing water at constant temperatures through the sample holder. The high temperature limit was set at 70°C to prevent thermal polymerization. The cure was achieved by using an Acticure® Ultraviolet/Visible Spot Cure System (EFOS, 250-450 nm band pass filter) with an effective irradiance of 100 mW/cm<sup>2</sup>, as measured by a radiometer (EFOS, R5000). The conversion ( $\alpha$ ) of each reactive moiety was calculated from the collected Raman spectra using

$$\alpha = 1 - \frac{A_{rxn}(t)}{A_{rxn}(0)} \quad (1.1)$$

where  $A_{rxn}(t)$  is the peak area of the reactive band at a given time,  $t$ , in the reaction, and  $A_{rxn}(0)$  is the peak area of the reactive band before the reaction begins. The reactive bands representing the acrylate C=C and the epoxide ring are located at 1640 cm<sup>-1</sup> and 790 cm<sup>-1</sup>, respectively.<sup>15</sup> Since the spectral baselines were constant throughout the experiment, a

reference band was not needed. Note that the conversion profiles presented have been smoothed using OriginLab 8.1 data analysis and graphing software. The smoothing used a 5 point Savitzky-Golay method in the conversion-time profile at different temperatures.

### Results and Discussion

The conversions of acrylate and epoxide functional groups of the hybrid monomer as a function of temperature are shown in Figure 2.2 and 2.3, respectively. In Figure 2.2, the methacrylate conversion increased from 0 to approximately 40s, then plateaued after 40s. The polymerization rate for the methacrylate increased as temperature increased from 30°C to 70°C, as indicated by the increased steepness of the conversion profile. In Figure 2.3, the epoxide ultimate conversion and corresponding polymerization rate increased with increasing temperature. The increased reaction rate is a result of enhanced molecular mobility at elevated temperatures, such as from reactive diffusion or thermal initiation as a result of autoacceleration.<sup>17</sup> Further studies would be needed to clarify the cause.

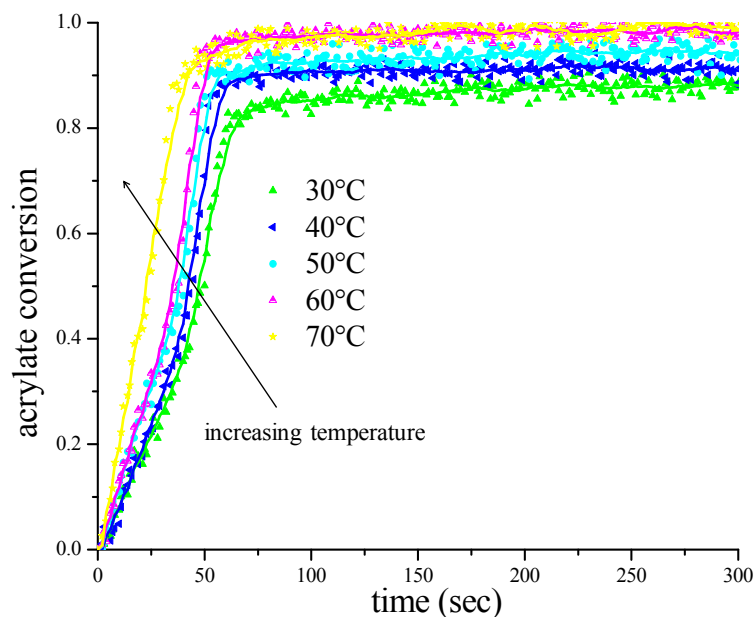


Figure 2.2: Acrylate C=C conversion for hybrid monomer METHHB with 0.17wt% DMPA and an effective irradiance of 100 mW/cm<sup>2</sup>

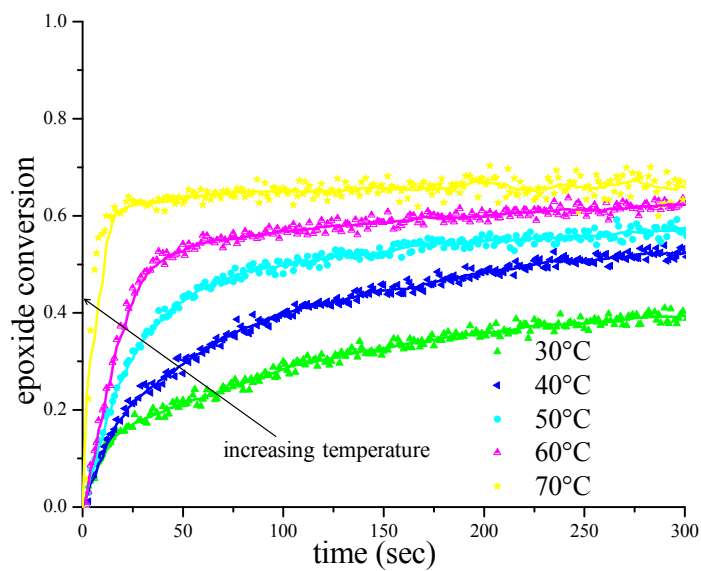


Figure 2.3: Conversion of epoxide ring for hybrid monomer, METHHB with 0.5 wt% DAI and an effective irradiance of 100 mW/cm<sup>2</sup>



Kinetic Rate Expressions  
Rate of Polymerization of Hybrid Monomer,  
METHB

The three major kinetic steps of radical chain polymerization (initiation, propagation, and termination) were described in Scheme 1.1. This kinetic analysis focuses the propagation rate for the monomer. The rate of propagation,  $R_p$ , for METHB can be expressed mathematically as a function of conversion ( $\alpha$ ) and time ( $t$ ) for acrylate and epoxide moieties by

$$R_p = -\frac{d[M]}{dt} \quad (2.1)$$

where the monomer concentration,  $[M]$ , can be expressed as a function of the initial monomer concentration,  $[M]_0$ , and the conversion:  $[M] = [M]_0(1 - \alpha)$ .

$$R_p = -\frac{d}{dt}[M]_0 + \frac{d\alpha}{dt}[M]_0 \quad (2.2)$$

Since  $\frac{d}{dt}[M]_0$  is 0, Equation 2.2 then becomes

$$R_p = \frac{d\alpha}{dt}[M]_0 \quad (2.3)$$

By taking the derivative of the conversion profiles in Figures 2.2 and 2.3 as a function of time and multiplying by  $[M]_0$ , the rate of polymerization is obtained (see Figures 2.4 and 2.5 for acrylate and epoxide moieties, respectively).

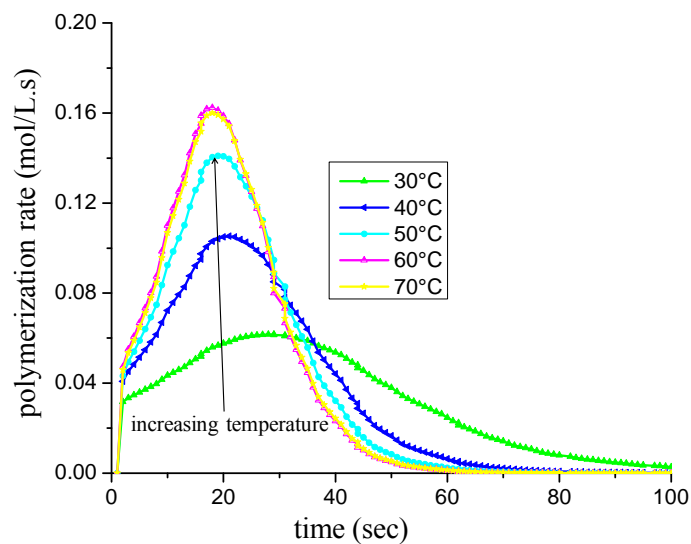


Figure 2.4: Acrylate C=C rate of polymerization for hybrid monomer, METHB with 0.17wt% DMPA and an effective irradiance of 100 mW/cm<sup>2</sup>

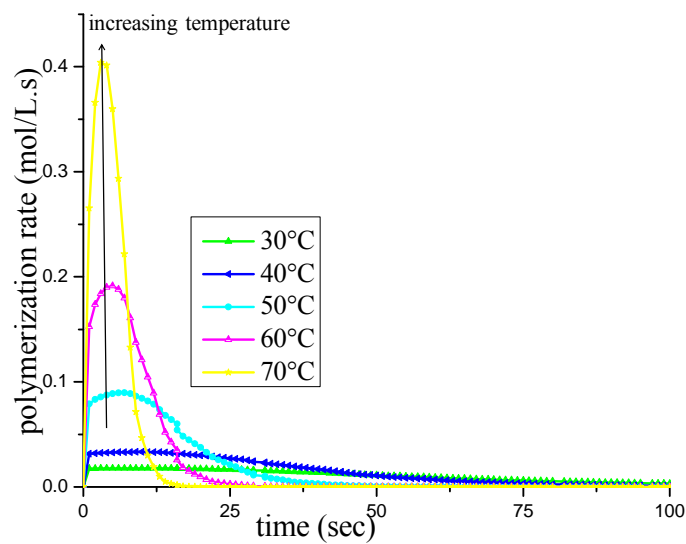


Figure 2.5: Epoxide rate of polymerization for hybrid monomer, METHB with 0.5 wt% DAI and an effective irradiance of 100 mW/cm<sup>2</sup>

In order to obtain the propagation rate constants,  $k_p$ , the rate of propagation of METHB can be derived from the kinetic rate expression for the propagation kinetic step

$$R_p = k_p[M][M^*] \quad (2.4)$$

where  $[M^*]$  is the concentration of propagating species, which for a general chain polymerization can be cationic, anionic, or free radical. Generally, it is difficult to measure the concentration of propagating chain species experimentally. Hence, assumptions have to be made for radical and cationic reactions.

To obtain an expression for the radical moiety of METHB, the quasi-steady-state assumption was made. The quasi-steady-state assumption states “that the concentration of radicals increases initially and almost instantaneously reaches a constant steady-state value. The rate of change of concentration of radicals quickly becomes zero and remains unchanged during the course of polymerization.”<sup>9</sup> For this free-radical photopolymerization, this assumption must be applied twice: once to derive an expression for the concentration of free-radical photoinitiator fragments,  $[R^*]$ , and once to derive an expression for the concentration of propagating chains,  $[M^*]$ . The latter can be developed mathematically from the kinetic rate expressions by equating the rates of initiation and termination,  $R_i$  and  $R_t$ , respectively:

$$R_i = 2I_a\Phi = R_t = 2k_t[M^*]^2 \quad (2.5)$$

where  $I_a$  is the absorbed light intensity, and  $\Phi$  is the number of propagating chains produced per photon absorbed (often called the quantum yield for initiation), and  $k_t$  is the termination rate constant.  $k_t$  was calculated experimentally according to a known method<sup>18</sup> to be  $1.32 \times 10^8$  L/(mol's) for the range of temperature 30°C to 70°C (see Appendix A.1 for detailed discussion). The two free radicals produced when DMPA photolyzes (see Figure 1.1.) are accounted for by the factor 2 in the expression for the rate of initiation, and the quantum yield,  $\Phi$ , for DMPA is 0.4.<sup>19</sup>

In bulk polymerization, the absorbed light intensity,  $I_a$ , is dependent upon factors such as sample thickness, light attenuation, and initiator concentration. This relationship can be simplified using the Beer-Lambert model, at a wavelength of 365 nm, and effective irradiance of 100mW/cm<sup>2</sup> and expressed as follows

$$I_a = I_0(1 - e^{-2.3\epsilon b[I]}) \quad (2.6)$$

where  $I_0$  is the incident light intensity,  $\epsilon$  is the molar absorptivity of the photoinitiator in L/(mole·cm),  $b$  is the thickness of reaction system in mm, and  $[I]$  is the photoinitiator concentration in mole/L. Here, the molar absorptivity of DMPA at  $\lambda = 365$  nm is 150 L/(mole·cm).<sup>20</sup> To simplify the calculations, other wavelengths were not considered for this analysis.

Hence, concentration of propagating chain species for a free-radical reaction can be expressed as<sup>21</sup>

$$[M\cdot] = \left( \frac{\Phi I_0(1 - e^{-2.3\epsilon b[I]})}{k_t} \right)^{0.5} \quad (2.7)$$

In a cationic reaction, the quasi-steady-state approximation is not valid since the concentration of cationic active centers changes over time and/or due to the lack of termination reactions. Although the mechanism and kinetics of cationic systems are not fully understood, studies have been carried out<sup>22</sup> to validate a generalization for the concentration of propagating species of cationic system, which is expressed as

$$[M^+] = \Phi \cdot [I]_0(1 - e^{-k_{abs} t}) \quad (2.8)$$

where  $[I]_0$  is the concentration of photoinitiator before illumination and  $k_{abs}$  is the absorption rate constant. The quantum yield,  $\Phi$ , and absorption rate constant for the cationic initiator DAI have been reported as 0.7 and  $0.027 \text{ s}^{-1}$ , respectively.<sup>22,23</sup>

#### Propagation Rate Constant of METHB

The concentration of propagating species, shown in Equations 2.7 and 2.8, can be substituted into Equation 2.4 to obtain expressions for the rate of propagation and the propagation rate constant, respectively, for the acrylate (Equations 2.9 and 2.10) and epoxide (Equations 2.11 and 2.12) moieties

$$R_p = k_p [M] \left( \frac{\Phi I_0 (1 - e^{-2.3\epsilon b [I]})}{k_t} \right)^{0.5} \quad (2.9)$$

$$k_p = \frac{R_p}{[M] \sqrt{\frac{\Phi I_0 (1 - e^{-2.3\epsilon b [I]})}{k_t}}} \quad (2.10)$$

$$R_p = k_p [M] \Phi \cdot [I]_0 (1 - e^{-k_{abs} t}) \quad (2.11)$$

$$k_p = \frac{R_p}{[M]\Phi \cdot [I]_0(1 - e^{-k_{abs} t})} \quad (2.12)$$

In Figures 2.4 and 2.5, the rate of polymerization increased with increasing reaction temperature. The propagation rate constant for methacrylate and epoxide was determined at the time of maximum conversion using Equations 2.10 and 2.12 to account for apparent propagation rate only. Each of the rate constants can be expressed by an Arrhenius-type relationship as shown in Equations 2.13 and 2.14 to obtain the apparent amount of energy required for the reaction to occur for the acrylate and epoxide moieties of the hybrid monomer, METHB. The apparent activation energy of propagation,  $E_p$ , and collision frequency factor,  $A_p$ , were determined from the slope and intercept, respectively, of  $\ln k_p$  versus  $1/T$  plots, as shown in Figures 2.6 and 2.7.

$$k_p = A e^{-E_p/RT} \quad (2.13)$$

or

$$\ln k_p = \ln A - \frac{E_p}{RT} \quad (2.14)$$

where  $R$  is the ideal gas constant and  $T$  refers to the absolute temperature.

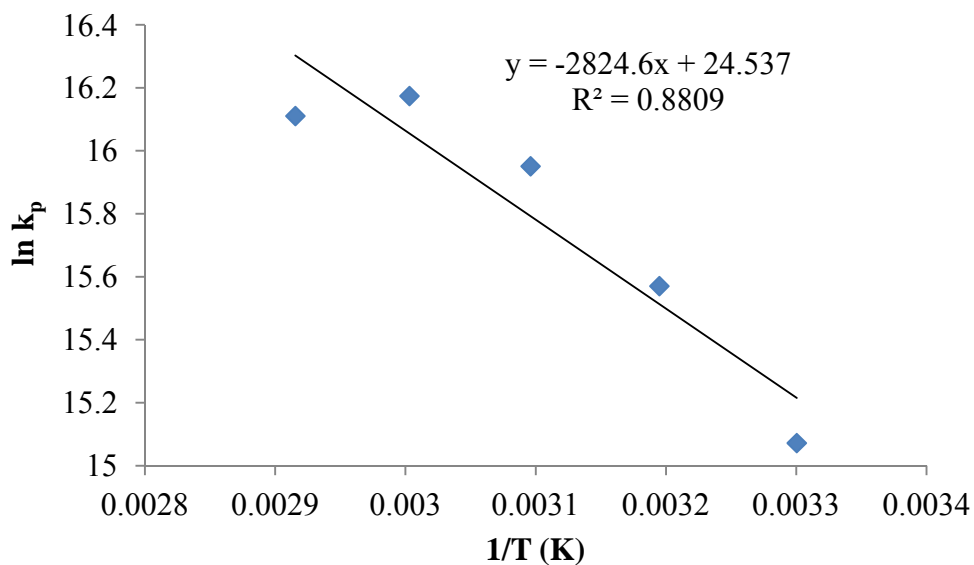


Figure 2.6: Arrhenius plot for the acrylate C=C in hybrid monomer, METHB with 0.17wt% DMPA and an effective irradiance of 100 mW/cm<sup>2</sup>.  $k_p$  (L/(mol·s)) was obtained from equation 2.10, by substituting for the respective variables.

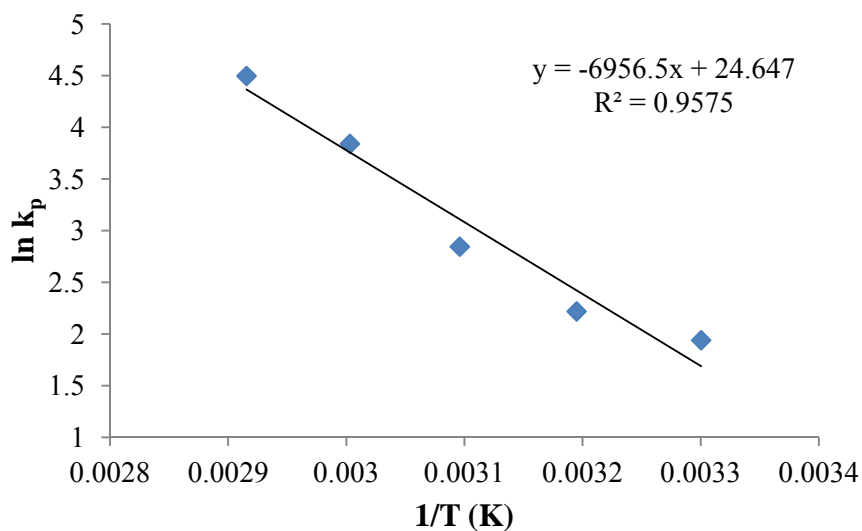


Figure 2.7: Arrhenius plot for the ring-opening polymerization of epoxide in hybrid monomer METHB with 0.5 wt% DAI and an effective irradiance of 100 mW/cm<sup>2</sup>.  $k_p$  (L/(mol·s)) was obtained from equation 2.12, by substituting for the respective variables.

The apparent activation energy of propagation obtained for the methacrylate C=C and the epoxide ring-opening polymerization from Figures 2.6 and 2.7 is 23.49 kJ/mol and 57.84 kJ/mol, respectively. The results obtained are comparable to those reported in the literature, for methacrylate, 22.36 kJ/mol and those for epoxides are listed in Table B1, for the respective acrylate and epoxide moieties. The frequency factor for the methacrylate is  $4.532 \times 10^{10}$  L/(mol·s) and for the epoxide is  $5.059 \times 10^{10}$  L/(mol·s). The goodness of fit in Figure 2.6 and 2.7 is less than unity because errors that might have arisen. The goodness of fit could be improved for the acrylate reaction by excluding 70°C data point, thereby limiting thermal auto-acceleration (see Figure 2.8). The resulting activation energy for methacrylate C=C from Figure 2.8 is 31.05 kJ/mol, and the frequency factor is  $8.353 \times 10^{11}$  L/(mol·s). A two percent improvement in the goodness of fit showed a 32% increase in the activation energy of the methacrylate reaction, indicating the impact of thermal excursion on the activation energy of polymerization.



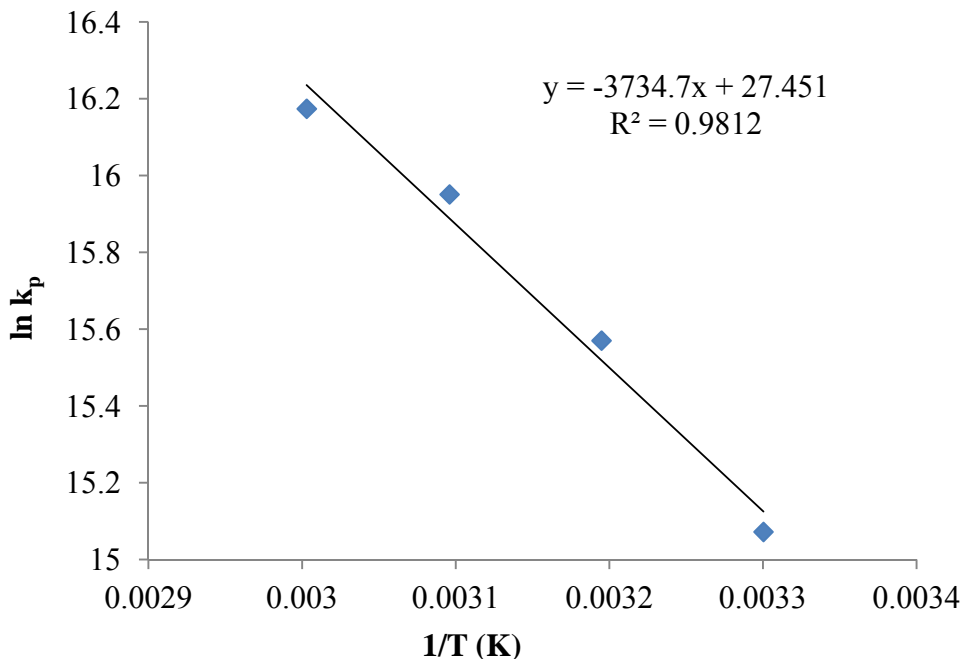


Figure 2. 8: Arrhenius plot for the acrylate C=C in hybrid monomer, METHB with 0.17wt% DMPA and an effective irradiance of 100 mW/cm<sup>2</sup>. The data point for 70°C has been removed.

In addition, the each data run was conducted only once, and the propagation rate constant was determined at the time of maximum conversion where diffusion is limited and auto-acceleration might be problematic.

### Conclusion

Raman spectroscopy was used to probe the kinetics of the hybrid monomer, METHB, which contains acrylate and epoxide moieties. The conversion was monitored in real time for sets of isothermal reactions ranging from 30°C to 70°C. The polymerization rates were determined for the acrylate and epoxide moieties. The concentration of the propagating chain for the acrylate moiety was determined through the quasi-steady state assumption and the epoxide moiety by cationic generalization. The kinetic rate constant was expressed by an Arrhenius-type relationship to obtain the activation energy of

propagation for methacrylate C=C of 23.49 kJ/mol and epoxide ring opening of 57 kJ/mol. The frequency factor for the methacrylate is  $4.53 \times 10^{10}$  L/mol.s and for the epoxide is  $5.06 \times 10^{10}$  L/mol.s.

### Notes

1. Zak, G.; Sela, M.N.; Yevko, V.; Park, C.B.; Benhabib, B. Layered-Manufacturing of Fiber-Reinforced Composites. *Journal of Manufacturing Science and Engineering*. 1999;121:448-456.
2. Fouassier, J.P. Photopolymerization Reactions Under Visible Lights: Principle, Mechanisms and Examples of Applications. *Progress in organic coatings*. 2003;47:16-36.
3. Moussa, K.; Decker, C. Light-Induced Polymerization of New Highly Reactive Acrylic Monomers. *Journal of Polymer Science Part A: Polymer Chemistry*. 1993;31:2197-2203
4. Wei, H.; Li, Q.; Ojelade, M.; Madbouly, S.; Otaigbe, J.U.; Hoyle, C.E. Thiol-Ene Free-Radical and Vinyl Ether Cationic Hybrid Photopolymerization. *Macromolecules*. 2007;40:8788-8793.
5. Lin, Y.; Stansbury, J.W. Kinetics Studies of Hybrid Structure Formation by Controlled Photopolymerization. *Polymer*. 2003;44:4781-4789.
6. Decker C. UV-radiation curing of acrylate/epoxide systems. *Polymer*. 2001;42:5531-5541.
7. Cai, Y.; Jessop, J.L.P. Decreased Oxygen Inhibition in Photopolymerized Acrylate/Epoxide Hybrid Polymer Coatings as Demonstrated by Raman Spectroscopy. *Polymer*. 2006;47:6560-6566.
8. Lin, Y.; Stansbury, J.W. The Impact of Water on Photopolymerization Kinetics of Methacrylate/vinyl Ether Hybrid Systems. *Polymer Advanced Technologies*. 2005;16:195-199.
9. Odian, G.G. *Principles of Polymerization / George Odian*. (Fourth Edition edition). New York: Wiley, 2004. Page 204-207, 271
10. Tryson, C.R.; Shultz A.R. A Calorimetric Study of Acrylate Photopolymerization. *Journal of Polymer Science: Polymer Physics Edition*. 1979;17:2059-2075.
11. Chien, J.C.W.; Cheun, Y.; Lillya, C.P. Cationic Polymerizations of Dioxepane and Its 2-Alkyl Derivatives. *Macromolecules*. 1988;21:870-875.
12. Dreyfuss, P.; Dreyfuss, M.P. *Chapter 4 Polymerization of Cyclic Ethers and Sulphides. /: . Comprehensive Chemical Kinetics*. Elsevier:259-330.
13. Sims, D. Polymerisation of tetrahydrofuran (part II). *Die Makromolekulare Chemie*. 1966;98:235-244.

14. He, Y.; Xiao, M.; Wu, F.; Nie, Jun. Photopolymerization Kinetics of Cycloaliphatic Epoxide-Acrylate Hybrid Monomer. *Polymer International*. 2007;56:1292-1297.
15. Cai, Y.; Jessop J.L.P. Effect of Water Concentration on Photopolymerized Acrylate/Epoxide Hybrid Polymer Coatings as Demonstrated by Raman Spectroscopy. *Polymer*. 2009;50:5406.
16. Beuermann, S.; Buback, M.; Davis, T.P, Gilbert, R.G.; Hutchinson, R.A.; Olaj, O.F.; Russel, G.T.; Schweer, J.; Alex, M.H. Critically Evaluated Rate Coefficients for Free-Radical Polymerization, 2. Propagation Rate Coefficients for Methyl Methacrylate. *Macromolecular Chemistry and Physics*. 1997;198:1545-1560.
17. Decker, C.; Decker, D.; Morel, F. Light Intensity and Temperature Effect in Photoinitiated Polymerization. *American Chemical Society Symposium Series*. 1997:63-63
18. Yanada, B.; Kobatake, S.; Aoki, S. Rate Constants for Elementary Reactions of the Radical Polymerization of Methyl 2-(Benzyloxymethyl)Acrylate as Polymerizable Acrylate Bearing Large Substituents. *Macromolecular Chemistry and Physics*. 1994;195:933-942.
19. Decker, C. Photoinitiated Crosslinking Polymerization. *Progress in Polymer Science*. 1996;21:593-650.
20. Burdick, J.; Lovestead, T.M.; Anseth, K.S. Kinetic Chain Lengths in Highly Cross-linked Networks Formed by the Photoinitiated Polymerization of Divinyl Monomers: A Gel Permeation Chromatography Investigation. *Biomacromolecules*. 2003;4:149.
21. Andrzejewska, E. Photopolymerization Kinetics of Multifunctional Monomers. *Progress in polymer science*. 2001;26:605-665.
22. Sipani, V.; Scranton, A.B. Dark-Cure Studies of Cationic Photopolymerizations of Epoxides: Characterization of the Active Center Lifetime and Kinetic Rate Constants. *Journal of polymer science. Part A, Polymer chemistry*. 2003;41:2064-2072
23. Sipani, V.; Kirsh, A.; Scranton, A.B. Dark cure Studies of Cationic Photopolymerizations of Epoxides: Characterization of Kinetic Rate Constants at High Conversions. *Journal of polymer science. Part A, Polymer chemistry*. 2004;42:4409-4416.

## CHAPTER 3

CONVERSION ENHANCEMENT AND PHYSICAL  
PROPERTY CONTROL IN EPOXIDE-ACRYLATE  
HYBRID PHOTOPOLYMERIZATIONS WITH  
HYDROXYL-CONTAINING ACRYLATESIntroduction

Hybrid photopolymerizations, which contain two functional groups polymerized by independent reaction mechanisms, have arisen in recent years. Free-radical and cationic photopolymerization systems such as acrylate-cyclic ethers,<sup>1-3</sup> thiol-ene/vinyl ether,<sup>4</sup> and acrylate-vinyl ether<sup>5-7</sup> hybrid systems have been reported. The hybrid resins may consist of a hybrid monomer, which combines the two functional groups in a single monomer, or hybrid mixture, in which the two functional groups are on separate molecules.

Acrylate-epoxide hybrid systems have been developed<sup>1</sup> to reduce atmospheric sensitivity to oxygen and humidity<sup>8</sup> and to enable sequential cure.<sup>2</sup> High polymerization shrinkage that results from acrylate moieties<sup>9,10</sup> is reduced in epoxy-acrylate hybrid resins because epoxides result in lower or no shrinkage during polymerization with respect to acrylates.<sup>11</sup>

Despite the advantages of epoxy-acrylate hybrid resins, problems persist that must be addressed. For example, polymers from hybrid monomers such as 3,4-epoxy-cyclohexylmethyl methacrylate (METHB) are brittle, due to the high cross-linking density that results from the short distance between the acrylate and epoxide moieties on the molecule. Hybrid mixtures of acrylates and epoxide moieties could mitigate this problem; however, phase separation then becomes a concern.<sup>12,13</sup> Most problematic is the low conversions and slow curing rates of epoxides in the hybrid systems. The much faster

acrylate reaction creates its polymer domains first, thereby preventing the epoxide from achieving high conversion.<sup>1</sup>

An examination of the epoxide chain growth mechanisms provides a possible solution to this problem of low epoxide conversions and slow curing rates. Propagation of the cationically polymerizable epoxides proceeds through the active chain end (ACE) mechanism,<sup>14</sup> shown in Scheme 1.4a. However, a second mechanism, the activated monomer (AM) mechanism, occurs in the presence of a nucleophilic species, such as an alcohol (Scheme 1.4b). In this chain transfer reaction, a proton is released rapidly between proton donors present in the system, which can activate an epoxide to start a new epoxide polymer chain.<sup>15</sup> ACE mechanisms are known to result in slow propagation, which accounts for the low conversion of epoxides; however, it has been found that the propagation rate for the AM mechanism is typically five times higher than the ACE mechanism.<sup>16</sup>

The hypothesis of this study is that hydroxyl-containing acrylates in epoxy-acrylate hybrid formulations will result in increased epoxide rate of polymerization and conversion through promotion of the AM mechanism. Facilitation of the AM mechanism will also covalently bond the epoxide network to the acrylate chain through the hydroxide contained in the acrylate, thereby reducing phase separation. The  $T_g$  is lowered when an acrylate is chosen with a lower  $T_g$  than the epoxide. Here, the acrylate content in the hybrid formulations is varied to control the extent of these reactions and to examine their effect on the kinetics and polymer properties.

## Experimental

### Materials

Epoxide-acrylate hybrid formulations were made by varying the content of 3,4-epoxycyclohexane carboxylate (EEC, Union Carbide) from 17 to 100 wt% and 2-hydroxyethyl acrylate (HEA, Union Carbide) from 17 to 100 wt% and 2-hydroxyethyl acrylate (HEA, BASF) from 50 to 100 wt%, respectively. HEA was used to promote the AM mechanism, and ethylene glycol methyl ether acrylate (EGMEA, BASF) was used as a non-hydroxyl-containing control. Formulations contained 0.5 wt% diaryliodonium hexafluoroantimonate (DAI, Sartomer). Upon photolysis, this photoinitiator produces both cationic and free-radical active centers for the epoxide and acrylate polymerizations in this study, respectively.<sup>18</sup> All materials were used as received and are shown in Figure 3.1.

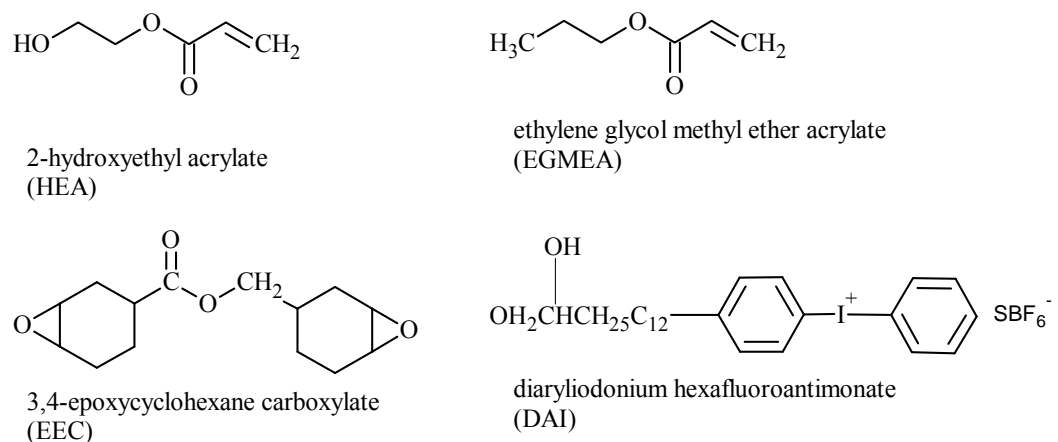


Figure 3.1: Molecular structures of monomers and photoinitiator used in this study

## Methods

### Kinetic Studies using Raman Spectroscopy

Raman spectroscopy was used to monitor the rate of photopolymerization and conversion of epoxide and acrylate moieties in real time. A 785-nm near-infrared laser was used to induce the Raman scattering effect, and the Mark II holographic fiber-coupled stretch probehead (Kaiser Optical Systems, Inc.) attached to the HoloLab 5000R modular research Raman spectrograph was used to obtain spectra of the hybrid formulations during photopolymerization. The exposure time for spectra was 200 ms. Samples were cured isothermally at 30°C in 1-mm ID quartz capillary tubes using an Acticure® Ultraviolet/Visible Spot Cure System (EFOS, 250-450 nm band pass filter) with an effective irradiance of 100 mW/cm<sup>2</sup> as measured by a radiometer (EFOS, R5000). The conversion ( $\alpha$ ) of each reactive moiety was calculated from the collected Raman spectra using

$$\alpha = 1 - \frac{A_{rxn}(t)}{A_{rxn}(0)} \quad (1.1)$$

where  $A_{rxn}(t)$  is the peak area of the reactive band at a given time,  $t$ , in the reaction and  $A_{rxn}(0)$  is the peak area of the reactive band before the reaction begins. The reactive bands representing the acrylate C=C double bond and epoxide ring are located at 1640 and 790 cm<sup>-1</sup>, respectively.<sup>19</sup> Since the spectral baselines were constant throughout the experiment, a reference band was not needed. The data presented have been smoothed using OriginLab 8.1 data analysis and graphing software. The smoothing used a 15 points



Savitzky-Golay method to remove noise in the data at high conversion, when concentration of epoxide rings was low.

#### Physical Property Studies using Dynamic Mechanical Analysis

Polymer samples were prepared and tested to obtain glass transition temperature ( $T_g$ ) and storage modulus using dynamic mechanical analysis (DMA). Formulations were sandwiched between two glass slides, which were coated with Rain-x to prevent the polymer sample from sticking to the glass surface. Glass cover slips were used as spacers to achieve 300  $\mu\text{m}$  thickness. Samples contained in slides were illuminated for 15 min using Acticure® Ultraviolet/Visible Spot Cure System (EFOS, 250-450 nm band pass filter) with an effective irradiance of 100  $\text{mW}/\text{cm}^2$ . The polymerized samples, still between the glass slides, were passed through a Fusion UV system (BF9H2, UV-bulb) at 2 ft/min belt speed to ensure complete cure. After removal from the glass slides, the polymer samples were placed in an oven at 150°C for 2 hours to ensure thermal cure would not take place during the DMA experiments. Rectangular samples of approximately 15 mm length x 6.0 mm width x 0.30 mm thickness were cut from the polymer and placed in a DMA (Q800, TA) for the experiments. The storage modulus and  $\tan \delta$  values were recorded and plotted against temperature for the DMA multi-frequency strain mode, with dynamic amplitude of 15  $\mu\text{m}$  and a tension film clamp. The thermal events analyzed by the DMA were for a 1 Hz oscillating frequency at 3°C/min scan rate from -50°C or below to 350°C.

## Results and Discussion

This study investigated the effect of facilitating AM mechanism in epoxide-acrylate hybrid formulation on kinetic and physical properties of acrylate and epoxide polymerization, using only cationic initiator, DAI. It is known that the radical active centers generated during the cationic decomposition of DAI are suitable for initiating the free-radical reaction of acrylates at suitable reaction conditions. The reactions were studied by real-time Raman spectroscopy, and the physical properties of the coatings cured in ambient condition were investigated by dynamic mechanical analysis. Refutas equation was used to predict the viscosity of the hybrid mixture in order to account for the impact of viscosity during polymerization.

### Free-Radical Photopolymerization of Epoxy-Acrylate Hybrid Formulations

Conversion profiles for acrylate polymerization were obtained by Raman spectroscopy as a function of increasing epoxide concentration in the hybrid formulations containing only cationic photoinitiator. In Figure 3.2, the acrylate conversion of the neat EGMEA begins immediately, but levels off at 8% conversion after 25 s of illumination. The low conversion of the neat EGMEA is attributed to dissolved oxygen in the formulation, which immediately consumed radical active centers generated by cationic initiator, DAI. However, as EEC was introduced into the system, the acrylate conversion jumped from 8% to about 84% after 5 min. Similarly, the conversion decreased slightly as EEC concentration increased, which may be attributed to dilution effect of the EGMEA monomer in the formulation.

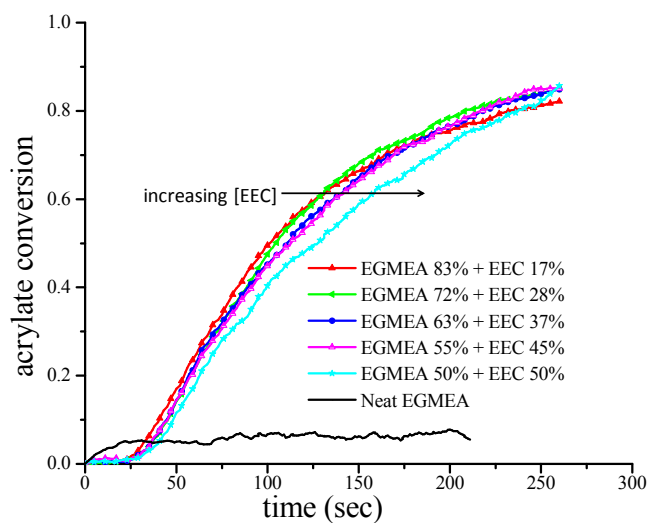


Figure 3.2: Acrylate C=C conversion for hybrid formulations of EEC-EGMEA (on a wt% basis) with 0.5 wt% DAI at 30°C and with an effective irradiance of 100 mW/cm<sup>2</sup>

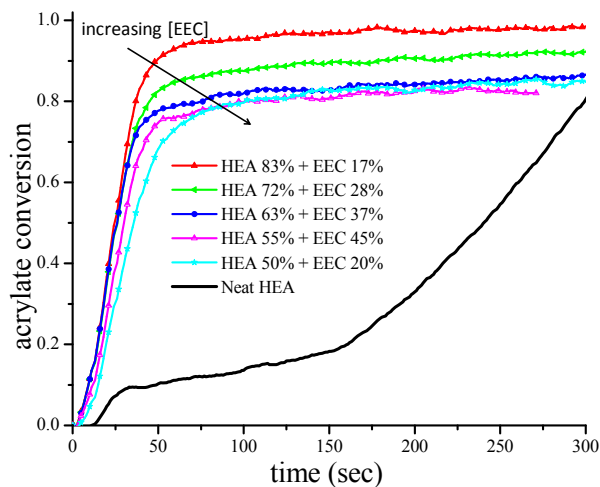


Figure 3.3: Acrylate C=C conversion for hybrid formulations of EEC-HEA (on a wt% basis) with 0.5 wt% DAI at 30°C and with an effective irradiance of 100 mW/cm<sup>2</sup>

In Figure 3.3, the presence of the hydroxyl group on the acrylate monomer produced a much higher acrylate conversion and rate of photopolymerization. The high

conversion and rate of polymerization for these hydroxyl-containing monomers are facilitated by hydrogen bonding, which mitigates termination reactions due to reduced polymer radical mobility.<sup>20</sup> The conversion and rate of polymerization for the neat HEA was delayed for 10 s, then reaches 20% conversion after 150 s of illumination and underwent auto-acceleration to reach 80% conversion. The initial delay was due to diffused oxygen: as the polymerization proceeded, the diffused oxygen was consumed in the system, leading to an increased acrylate conversion.<sup>21,22</sup> The polymerization rate of acrylate in the hybrid formulations began almost immediately and reached 80-95% conversion. In the hybrid formulations, reaction was complete within the first 50s of illumination; increasing EEC concentration reduced ultimate conversion. The increase in acrylate conversion in the hybrid formulation is attributed to hydrogen bonding effect between the acrylate and the hydroxyl group present.<sup>23</sup> Similarly, a dilution effect, resulting from low viscosity of the acrylate, facilitated higher acrylate conversions at low EEC concentrations.

To investigate the dilution effect, the viscosities of EEC-EGMEA and EEC-HEA mixtures were predicted using the Refutas equation (Equation 3.1),<sup>24</sup> and the results are shown in Figures 3.4 and 3.5. The EEC-EGMEA formulations have lower viscosities compared to the EEC-HEA formulations, however, the acrylate and Epoxide conversions are lower for the EEC-EGMEA formulation as compared to the EEC-HEA formulations.

$$\eta_{mixture} = e^{e^{\left(\frac{VBI_{mixture} - 10.975}{14.534}\right)}} - 0.8 \quad 3.1$$

where

$$VBI_{mixture} = [W_1 \times VBI_{comp,1}] + [W_2 \times VBI_{comp,2}] \quad 3.01$$

and

$$VBI_{comp} = 14.534 \times \ln[\ln(\eta_{comp} + 0.8)] + 10.975 \quad 3.02$$

The viscosity blending index ( $VBI$ ) for mixture and components is represented by  $VBI_{mixture}$  and  $VBI_{comp}$ . Viscosity of mixture and components in centipoises is represented by  $\eta_{mixture}$  and  $\eta_{comp}$ . Weight fraction of monomers in the mixture is represented by  $W_1$  and  $W_2$ .

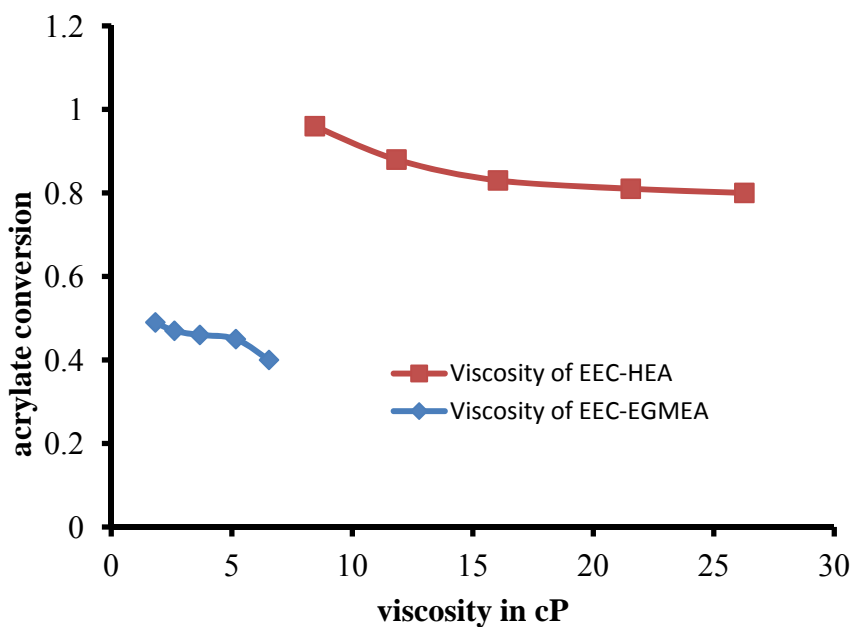


Figure 3.4: Acrylate conversion versus monomer viscosity in hybrid formulation of EEC-HEA and EEC-EGMEA. Viscosity of monomer composition is estimated using Refutas equation

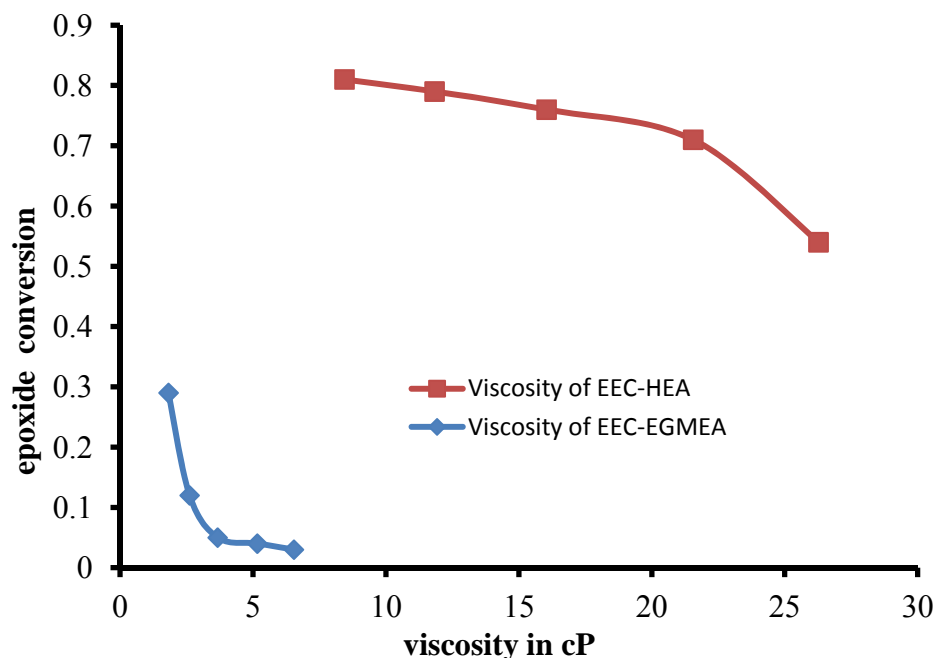


Figure 3.5: Epoxide conversion versus monomer viscosity in hybrid formulation of EEC-HEA and EEC-EGMEA. Viscosity of monomer composition is estimated using Refutas equation

#### Cationic Ring-Opening Photopolymerization of Epoxy-Acrylate Hybrid Formulations

Conversion profiles for epoxide polymerization were obtained by Raman spectroscopy as a function of increasing epoxide concentration in the hybrid formulations containing only cationic photoinitiator. The cationic photopolymerization was monitored simultaneously with the free-radical reaction, and the epoxide conversion and polymerization rate results are presented in Figures 3.6 and 3.7 for EEC-EGMEA and EEC-HEA formulations, respectively.

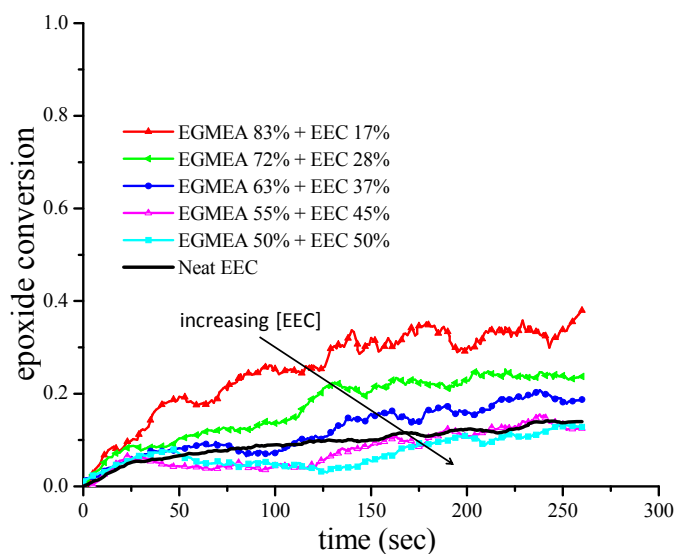


Figure 3.6: Conversion of epoxide ring for hybrid formulations of EEC-EGMEA (on a wt% basis) with 0.5 wt% DAI at 30°C and with an effective irradiance of 100 mW/cm<sup>2</sup>.

In Figure 3.6, the ring opening polymerization of the cationic monomer, EEC, proceeded through the active chain end (ACE) mechanism. As a result, the epoxide conversion and polymerization rates for the formulation were low. The initial rate of polymerization was the same in the hybrid formulation containing EEC concentrations higher than 37wt% as with the neat EEC system. However, conversion up to 40% was achieved after 250 s of illumination with hybrid formulations containing the lowest EEC concentration. Conversion of epoxide decreased from 40% to 15% with increasing EEC concentration. The increase in epoxide conversion at low EEC concentration can be attributed to the dilution effect of the acrylate monomer, EGMEA. The acrylate monomer EGMEA decreased the viscosity of the formulation with increasing acrylate concentration as shown in Figure 3.5.

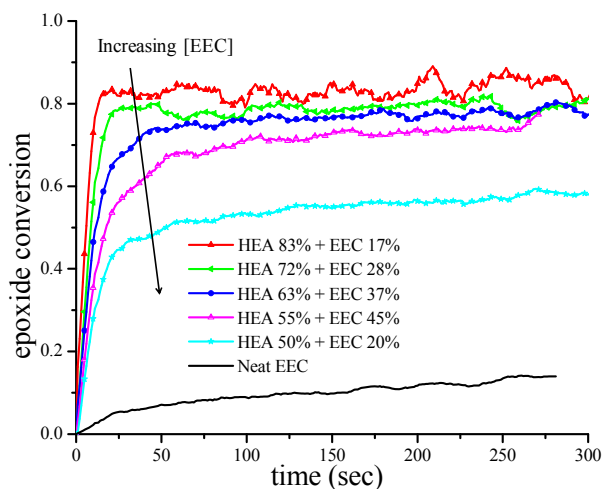


Figure 3.7: Conversion of epoxide ring for hybrid formulations of EEC-HEA (on a wt% basis) with 0.5 wt% DAI at 30°C and with an effective irradiance of 100 mW/cm<sup>2</sup>.

In Figure 3.7, the initial rate of polymerization was much faster for all hybrid formulations. Conversions up to 80% were reached after 50 s of illumination with all hybrid formulations. The ultimate conversions decreased from 80% to 60% with increasing EEC concentration, but are well above the neat system. The conversion of the neat EEC proceeded by the ACE mechanism, leading to a low conversion and rate of polymerization. However, as HEA was introduced into the system, the AM mechanism was facilitated, leading to a drastic increase from 17% conversion for the neat epoxide to 80% conversion in the hybrid formulation containing 17wt% EEC. The hydroxyl-containing acrylate, HEA, was the source of the chain transfer agent that facilitated the activated monomer (AM) mechanism, which was responsible for the increased epoxide conversion. The acrylate polymer chains and epoxide crosslinked network were also covalently bonded, through the hydroxyl groups in the acrylate, and this bonding provided an opportunity to tune the physical properties of the polymer.



### Physical Properties of Epoxide-Acrylate Hybrid Photopolymers

The EEC-EGMEA formulations were characterized by low acrylate and epoxide conversion. Thus, the physical properties of the polymers were so poor, that specimens could not be made for DMA measurements. Free-radical initiator DMPA was added to the formulation in order to obtain the representative  $\tan \delta$  data for EEC-EGMEA shown in Figure 3.8. However, as AM mechanisms were facilitated, the conversion of acrylate and epoxides increased, as shown in Figures 3.3 and 3.7. The covalent bonds between the acrylate and epoxide polymer systems resulted in a good polymer properties. Hence, the  $\tan \delta$  of EEC-HEA formulations with only the cationic photoinitiator DAI is presented in Figure 3.9.

As EEC concentration increased, the  $\tan \delta$  peak broadened from a narrow peak centered at  $-2^{\circ}\text{C}$  in the formulation containing 17wt% EEC and 83wt% of EGMEA to a very broad peak ranging from  $-25^{\circ}\text{C}$  to  $100^{\circ}\text{C}$  in the formulation containing 50wt% EEC and 50wt% EGMEA. The glass transition temperature of neat EEC was  $210^{\circ}\text{C}$ . The broadness in peak of the EEC-EGMEA formulations is an indication of phase separation occurring in the polymer as the EGMEA and EEC.

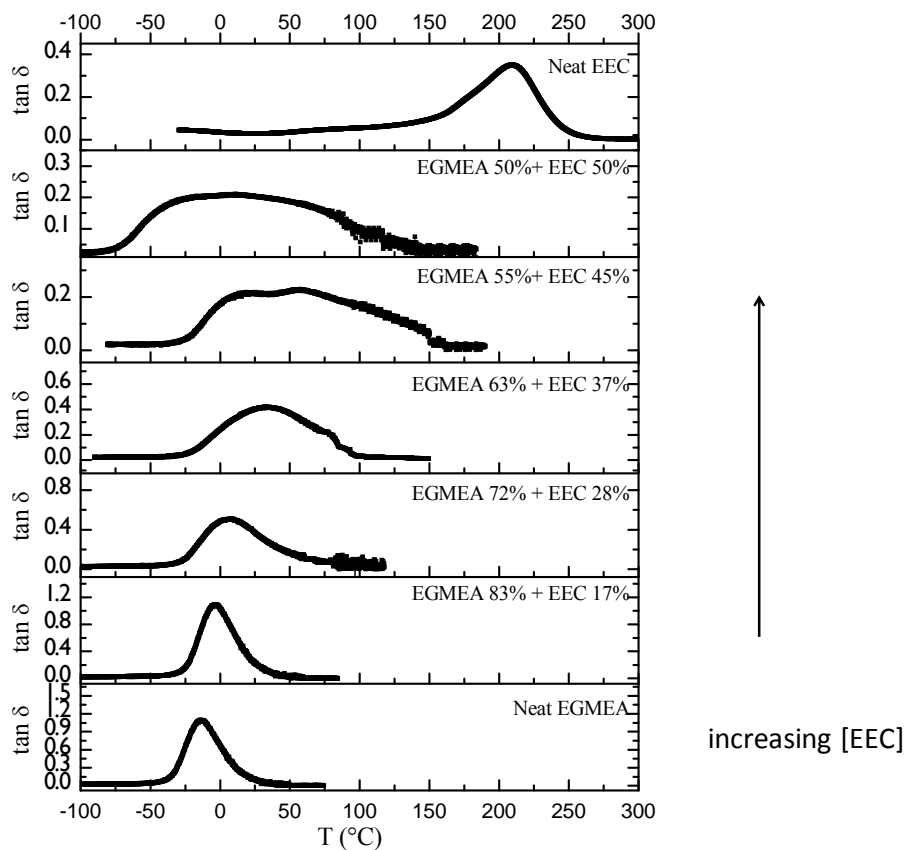


Figure 3.8: Tan  $\delta$  plots, obtained by DMA, of EEC-EGMEA polymers. Hybrid formulations were photopolymerized with 0.5wt% DAI and 0.017 wt% DMPA at 30°C for 15 min using an effective irradiance of 100 mW/cm<sup>2</sup>, and the resulting polymers were heat treated at 150°C for 2 hours.

However, when EGMEA was replaced by the hydroxyl-containing HEA in the formulations, the  $T_g$  of the hybrid polymers increased as the EEC concentration increased. In the formulation containing 17wt% EEC and 83wt% HEA, the  $T_g$  was 70°C, while the  $T_g$  was 93°C in the formulation containing 50wt% EEC and 50wt% HEA. As the acrylate concentration increased, the left-hand shoulder of the tan  $\delta$  peak disappeared, indicating reduced phase separation as the EEC and acrylate polymer domains were covalently connected through the hydroxyl group via the AM mechanism. Thus, low toughness of epoxides can be reduced by judiciously incorporating hydroxyl-containing

acrylates with the desired flexibility. Polymers from neat HEA were not obtained because the reaction was plagued with oxygen inhibition such that suitable specimens for DMA analysis were not obtained.

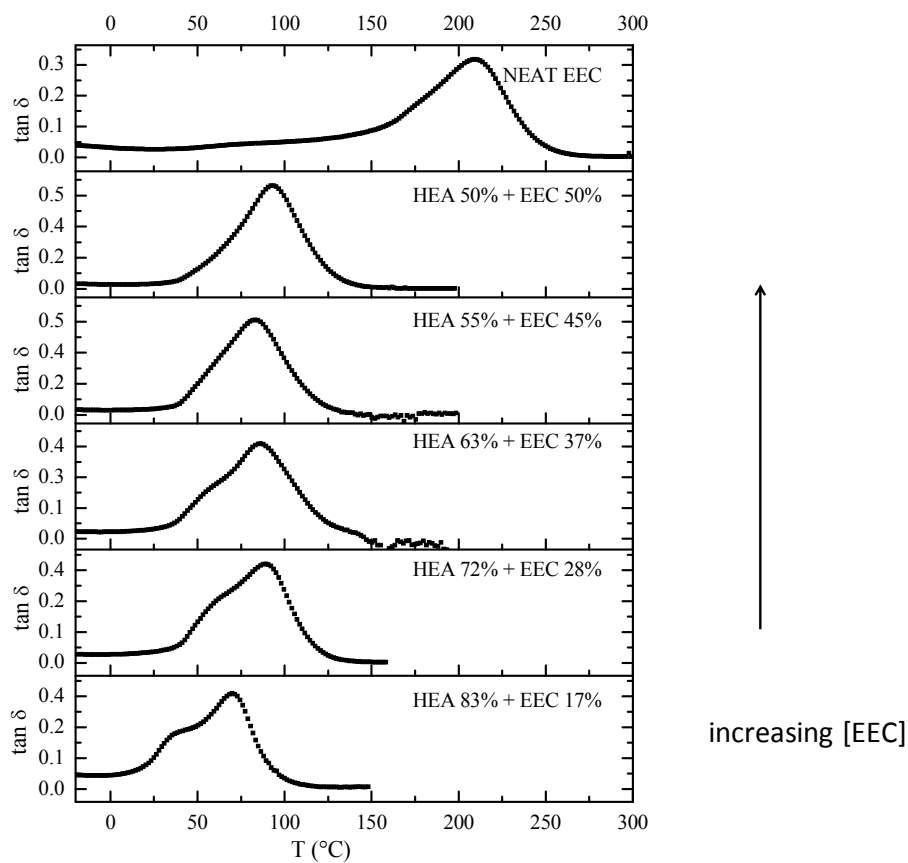


Figure 3.9:  $\tan \delta$  plots, obtained by DMA, of EEC-HEA polymers. Hybrid formulations were photopolymerized with 0.5wt% DAI at 30°C for 15 min using an effective irradiance of 100 mW/cm<sup>2</sup>, and the resulting polymers were heat treated at 150°C for 2 hours.

### Conclusions

Epoxide conversion and rate of polymerization in epoxide-acrylate hybrid monomer systems were shown to increase through the introduction of a hydroxyl group on the meth/acrylate monomer, taking advantage of the faster AM mechanism. In addition, this covalent bond linking the epoxide network to the meth/acrylate polymer chains resulted in little or no phase separation and a reduction of the  $T_g$  for the hybrid polymer compared to the neat epoxide.

Notes

1. Decker C. UV-radiation curing of acrylate/epoxide systems. *Polymer*. 2001;42:5531-5541.
2. Oxman, J.D.; Jacobs, D.W.; Trom, M.C.; Sipani, V.; Ficek, B.; Scranton, A.B. Evaluation of Initiator Systems for Controlled and Sequentially Curable Free-radical/Cationic Hybrid Photopolymerizations. *Journal of Polymer Science Part A: Polymer Chemistry*. 2005;43:1747-1756.
3. Crivello, J. Synergistic Effects in Hybrid Free Radical/Cationic Photopolymerizations. *Journal of Polymer Science. Part A, Polymer Chemistry*. 2007;45:3759.
4. Wei, H.; Li, Q.; Ojelade, M.; Madbouly, S.; Otaigbe, J.U.; Hoyle, C.E. Thiol-Ene Free-Radical and Vinyl Ether Cationic Hybrid Photopolymerization. *Macromolecules*. 2007;40:8788-8793.
5. Rajaraman, S.K.; Mowers, W.A.; Crivello, J.V. Interaction of Epoxy and Vinyl Ethers during Photoinitiated Cationic Polymerization. *J Polymer Science Part A*. 1999;37:4007-4018.
6. Lin, Y.; Stansbury, J.W. Kinetics Studies of Hybrid Structure Formation by Controlled Photopolymerization. *Polymer*. 2003;44:4781-4789.
7. Cho, J. UV-initiated Free-radical and Cationic Photopolymerizations of Acrylate/Epoxide and Acrylate/Vinyl Ether Hybrid Systems with and without Photosensitizer. *J Applied Polymer Science*. 2004;93:1473.
8. Cai, Y.; Jessop, J.L.P. Decreased Oxygen Inhibition in Photopolymerized Acrylate/Epoxide Hybrid Polymer Coatings as Demonstrated by Raman Spectroscopy. *Polymer*. 2006;47:6560-6566.
9. Williams, J.B.; Takeshi, E. Radical Ring-Opening Polymerization and Copolymerization with Expansion in Volume. *Journal of Polymer Science, Polymer Symposia*. 1978;64:17-26.
10. Leung, D.; Bowman, C.N. Reducing Shrinkage Stress of Dimethacrylate Networks by Reversible Addition-Fragmentation Chain Transfer. *Macromolecular chemistry and Physics*. 2012;213:198-204.
11. Sangermano, M.; Carbonaro, W.; Malucelli, G.; Priola, A. UV-Cured Interpenetrating Acrylic-Epoxy Polymer Networks: Preparation and Characterization. *Macromolecular Materials and Engineering*. 2008;293:515-520.

12. Russell, B.; Chartoff, R.; The Influence of Cure Conditions on the Morphology and Phase Distribution in a Rubber-Modified Epoxy Resin using Scanning Electron Microscopy and Atomic Force Microscopy. *Polymer*. 2005;46:785-798.
13. Duan, J.; Kim, C.; Jiang, P. On-line Monitoring of Cycloaliphatic Epoxy/Acrylate Interpenetrating Polymer Networks Formation and Characterization of their Mechanical Properties. *Journal of Polymer Research*. 2009;16:45-54.
14. Bednarek, M.; Kubisa, P.; Penczek, S. Coexistence of Activated Monomer and Active Chain End Mechanisms in Cationic Copolymerization of Tetrahydrofuran with Ethylene oxide. *Macromolecules*. 1999;32:5257-5263.
15. Ghosh, N.; Palmese, G. Electron-Beam Curing of Epoxy Resins: Effect of Alcohols on Cationic Polymerization. *Bulletin of Materials Science*. 2005;28:603-607.
16. Biedron, T.; Szymanski, R.; Kubisa, P.; Penczek, S. Kinetics of Polymerization by Activated Monomer Mechanism. *Makromolekulare Chemie-Macromolecular Symposia*. 1990;32:155-168.
17. Penczek, S.; Kubisa, P.; Szymanski, R. Activated Monomer Propagation in Cationic Polymerizations. *Makromolekulare Chemie-Macromolecular Symposia*. 1986;3:203-220.
18. Koleske, J.V. Cationic Photoinitiators and Initiation Mechanism. In: Radiation Curing of Coatings. Bridgeport, NJ: ASTM International, 2002:55-66.
19. Cai, Y.; Jessop, J.L.P. Effect of Water Concentration on Photopolymerized Acrylate/Epoxy Hybrid Polymer Coatings as Demonstrated by Raman Spectroscopy. *Polymer*. 2009;50:5406.
20. Lee, T.Y.; Roper, T.M.; Jonsson, S.E.; Guymon, C.A.; Hoyle, C.E. Influence of Hydrogen Bonding on Photopolymerization Rate of Hydroxyalkyl Acrylates. *Macromolecules*. 2004;37:3659-3665.
21. Studer, K.; Decker, C.; Schwalm, R. Overcoming Oxygen Inhibition in UV-curing of Acrylate Coatings by Carbon dioxide Inerting: Part II. *Progress in Organic Coatings*. 2003;48:101-111.
22. O'Brien, K.A.; Bowman, C.N. Modeling the Effect of Oxygen on Photopolymerization Kinetics. *Macromolecular Theory and Simulations*. 2006;15:176-182.
23. Lee, T.Y.; Guymon, C.A.; Jonsson, S.E.; Hoyle, C.E. The Effect of Monomer Structure on Oxygen Inhibition of (meth)acrylates Photopolymerization. *Polymer*. 2004;45:6155-6162.
24. Barabas, I.; Todorut, I. Predicting the Temperature Dependent Viscosity of Biodiesel-Diesel-Bioethanol Blends. *Energy Fuels*. 2011;25:5767-5774.

## CHAPTER 4

### CONCLUSIONS AND RECOMMENDATIONS

- Key kinetic constants for the hybrid monomer, METHB, were established in Chapter 2. In Chapter 3, it was demonstrated that epoxide conversion can be increased in hybrid formulations by incorporating a hydroxyl-containing acrylate. Using these results, further studies are recommended to control phase separation, physical properties, and shrinkage stress of these epoxy-acrylate polymers.
1. Increase epoxide conversion and rate of polymerization, by increasing the acrylate functionality, increasing the number of hydroxyls contained in the acrylate, changing the chemical structure of epoxides, in epoxy-acrylate hybrid formulation. A major setback in cationic reactions is the low polymerization rate and conversion of epoxides. The hybrid resins are not devoid of this setback; as such it is desired to achieve a high conversion of epoxide. Preliminary results have shown that epoxide conversion and rate of polymerization are increased when EEC is paired with hydroxyl-containing mono-acrylate. The hypothesis is that the activated monomer (AM) mechanism is facilitated. The new hypothesis is to increase epoxide conversion by changing the monomer structure such as increasing the acrylate functionalities, changing to different epoxides, increasing the hydroxides contained in the acrylates.
  2. Control phase separation in epoxy-acrylate hybrid resins. Phase separation is selective in its applications, for instance in impact resistance objects, phase separation is desired, while it is not in other applications. The hypothesis is that phase separation is controlled by changing the monomer composition of the hybrid resin in the presence of hydroxyl-containing acrylate, careful choice of initiator, for instance,

phase separation can be induced in a formulation when DAI only initiator is used, while the same formulation can become homogeneous when DMPA and DAI initiators are used.

3. Control physical properties of hybrid polymers. Understanding and controlling the mechanism of phase separation, chemical composition and nanostructure formation in polymers of epoxy-acrylate hybrid resins allows one to tailor the performance of the materials to a manifold of applications. It is hypothesized that the high glass transition temperature of the epoxide moiety can be used to increase thermal and mechanical properties such as toughness, stress at break or high-temperature creep resistance while retaining ease of processability stimulated by the acrylate moiety.
4. Reduce shrinkage stress in hybrid polymer materials by controlling the kinetics of photopolymerization. It is very desirable in many industrial applications to control the sequence of reaction in hybrid photopolymerization. It is hypothesized that a fast epoxide and slow acrylate conversions will result in low shrinkage stress and vice versa. This study facilitates the AM mechanism to achieve fast epoxide conversion, and subsequently induce ACE mechanism to retard the epoxide, to achieve fast acrylate conversion by controlling monomer concentration and initiator choice. Further discussion of shrinkage stress analysis is found in Appendix D.



APPENDIX A  
METHOD FOR ESTIMATION OF  $k_t$ .

**Materials:** The epoxide/methacrylate hybrid monomer 3,4-epoxy-cyclohexyl-methyl methacrylate (METHB, Diacel) (see Figure 2.1) was used in this study. 2,2-Dimethoxy-2-phenyl-acetophenone (DMPA, Aldrich) was used to initiate the free-radical (methacrylate) reaction. All materials were used as received.

**Method:** Raman spectroscopy was used to monitor the rate of photopolymerization and conversion of the methacrylate moiety in real-time. A 785-nm near-infrared laser was used to induce the Raman scattering effect. A Mark II holographic fiber-coupled stretch probehead (Kaiser Optical Systems, Inc.) attached to the HoloLab 5000R modular research Raman spectrograph was used to obtain spectra of the hybrid formulations during photopolymerization. The exposure time for each spectrum was 200 ms. Samples were isothermally cured at temperatures ranging from 30°C to 70°C in 1-mm ID quartz capillary tubes. The cure was achieved by using an Acticure® Ultraviolet/Visible Spot Cure System (EFOS, 250-450 nm band pass filter) with an effective irradiance of 100 mW/cm<sup>2</sup>, as measured by a radiometer (EFOS, R5000), and this initiation light was shuttered after 25 s of illumination. The conversion ( $\alpha$ ) of each reactive moiety was calculated from the collected Raman spectra using Equation 1.1. The reactive bands representing the acrylate C=C is located at 1640 cm<sup>-1</sup>, and since the spectral baselines were constant throughout the experiment, a reference band was not needed.

**Results:** The hybrid monomer METHB was photopolymerized using only the free-radical photoinitiator DMPA, and the initiating light was turned off at 25 sec for

isothermal reactions ranging from 30 to 70°C. The rate of polymerization that occurs in the dark can be expressed as

$$R_p = -\frac{d[M]}{dt} = k_p[M][P^\bullet] \quad (A1.1)$$

where  $[P^\bullet]$  is the concentration of propagating polymer chains. The rate of termination can be expressed as

$$R_t = -\frac{d[P]}{dt} = 2k_t[P^\bullet]^2 \quad (A1.2)$$

Equation A1.2 can be rearranged to the form

$$-\frac{d[P]}{[P^\bullet]^2} = 2k_t dt \quad (A1.3)$$

Integrating Equation A1.3, an expression for the concentration of propagating polymer chains

$$\frac{1}{[P^\bullet]} = 2k_t t + \frac{1}{[P^\bullet]_0} \quad (A1.4)$$

where  $[P^\bullet]_0$  is the concentration of the radicals at the beginning of the dark period and  $t$  is the time of dark reaction.

Equation A1.1 can be further rearranged to obtain

$$[P^\bullet] = \frac{R_p}{k_p[M]} \quad (A1.5)$$

By substituting Equation A1.5 into Equation A1.4, an estimate for  $\frac{2k_t}{k_p}$  can be obtained from the slope of the  $\frac{[M]}{R_p}$  versus  $t$  plot

$$\frac{[M]}{R_p} = \frac{2k_t}{k_p}t + \frac{[M]_0}{R_{p0}} \quad (\text{A1.6})$$

A plot of  $\frac{[M]}{R_p}$  of Equation A1.6 vs  $t$  yielded a straight line, with a slope of  $\frac{2k_t}{k_p}$ , for temperatures ranging from 30°C to 70°C.

Recall the rate of propagation as expressed by Equation 2.9

$$R_p = k_p[M] \left( \frac{\Phi I_0(1 - e^{-2.3\epsilon b[I]})}{k_t} \right)^{0.5} \quad (2.9)$$

Rearranging in terms of  $\frac{k_p}{\sqrt{k_t}}$  will yield

$$\frac{k_p}{\sqrt{k_t}} = \frac{R_p}{[M] \sqrt{\Phi I_0(1 - e^{-2.3\epsilon b[I]})}} \quad (\text{A1.7})$$

The value of  $\frac{k_p}{\sqrt{k_t}}$  can be estimated by substituting for the values in the RHS of equation A1.7 from the dark experiment.

If  $k_t$  is solved for in  $\frac{2k_t}{k_p}$  from  $\frac{k_p}{\sqrt{k_t}}$ , and the result expressed as a function of  $k_p$ , by iterating the results, the value of  $k_t$  and  $k_p$  were estimated as shown in Table A1 to be constant.

Table A1. Estimation of  $k_t$  from dark polymerization experiments.

Temperature (°C)	$\frac{2k_t}{k_p}$ From plot of $\frac{[M]}{R_p}$	$\frac{k_p}{\sqrt{k_t}}$ From equation A1.7	$k_p \times 10^{-5}$ L/(mol's)	$k_t \times 10^{-8}$ L/(mol's)
30	410.85	39.47	3.20	1.32
40	45.42	356.99	28.95	1.32
50	32.61	497.29	40.32	1.32
60	35.85	452.35	36.68	1.32
70	23.79	681.49	55.26	1.32

APPENDIX B  
LITERATURE VALUES FOR ACTIVATION  
ENERGIES OF CATIONIC RING-OPENING OF  
EPOXIDES

Table B1. Literature values for activation energies of cationic ring-opening of epoxides

Epoxide	Measurement Technique	Activation Energy (kJ/mol)	Reference
Oxetane	NMR	47	Dreyfuss and Dreyfuss, 1976
THF	Dilatometer	61	Sims, 1966
1,3-dioxolane	Gas Chromatography	49	Dreyfuss and Dreyfuss, 1976
Oxepane	Gas Chromatography	75	Chien et al., 1988
1,3-dioxepane	Gas Chromatography	86	Chien et al., 1988

THF (tetrahydrofuran), NMR (nuclear magnetic resonance)

## APPENDIX C

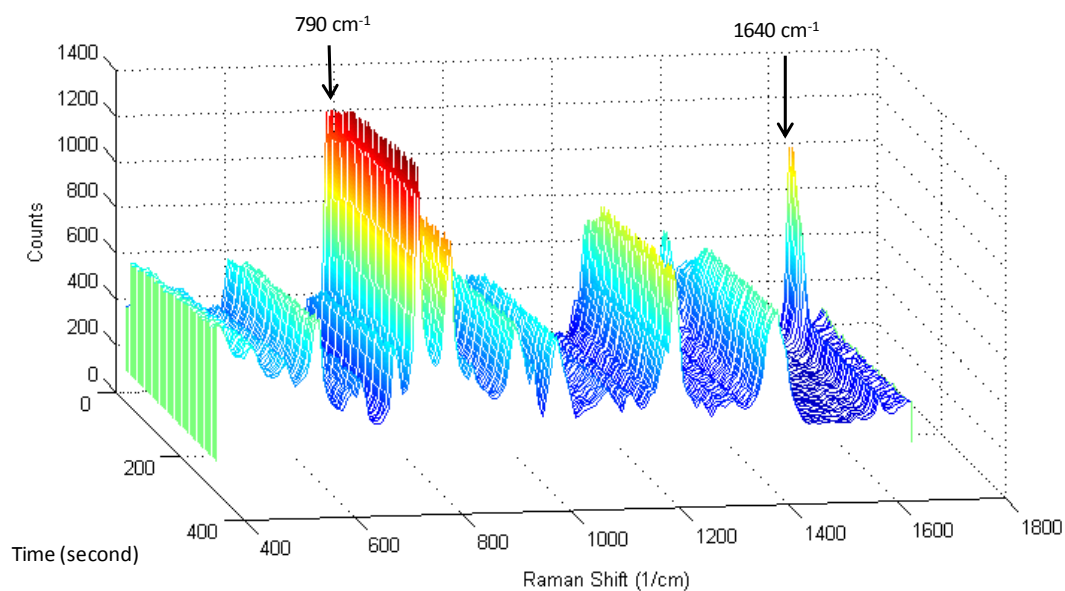
REPRESENTATIVE REAL-TIME RAMAN DATA FOR  
ISOTHERMAL PHOTOPOLYMERIZATIONS OF  
METHB IN CHAPTER 2

Figure C1: Real-time Raman waterfall plot of METHB with 0.17 wt% DMPA. Free-radical only photopolymerization with an effective irradiance of 100 mW/cm<sup>2</sup> at 30°C.

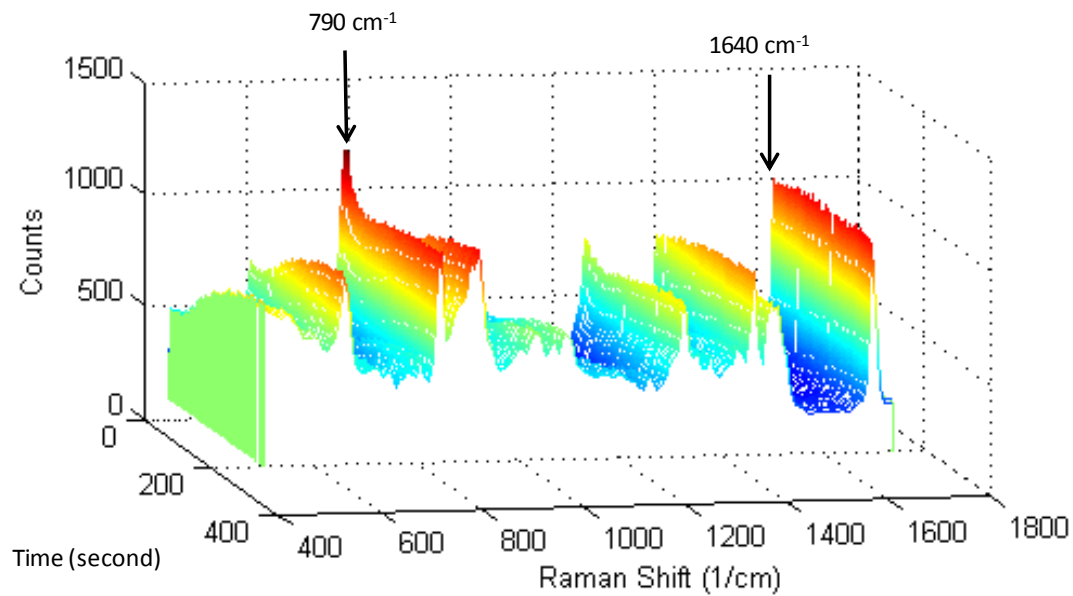


Figure C1: Real-time Raman waterfall plot of METHHB with 0.5 wt% DAI. Cationic only photopolymerization with an effective irradiance of 100 mW/cm<sup>2</sup> at 30°C.

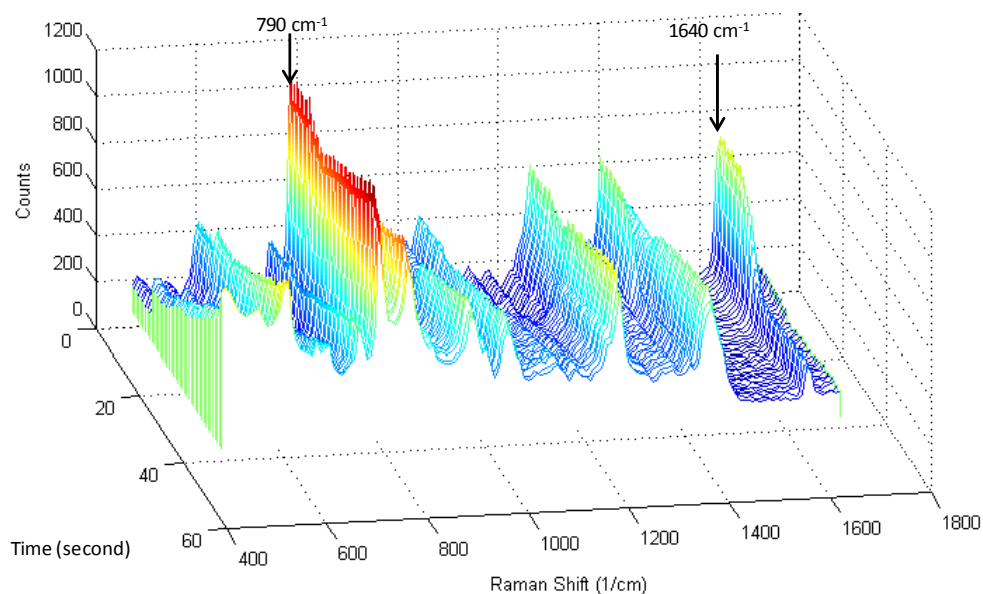


Figure C2: Real-time Raman waterfall plot of METHHB with 0.5 wt% DAI and 0.17 wt% DMPA. Free-radical and cationic photopolymerization with an effective irradiance of 100 mW/cm<sup>2</sup> at 30°C.

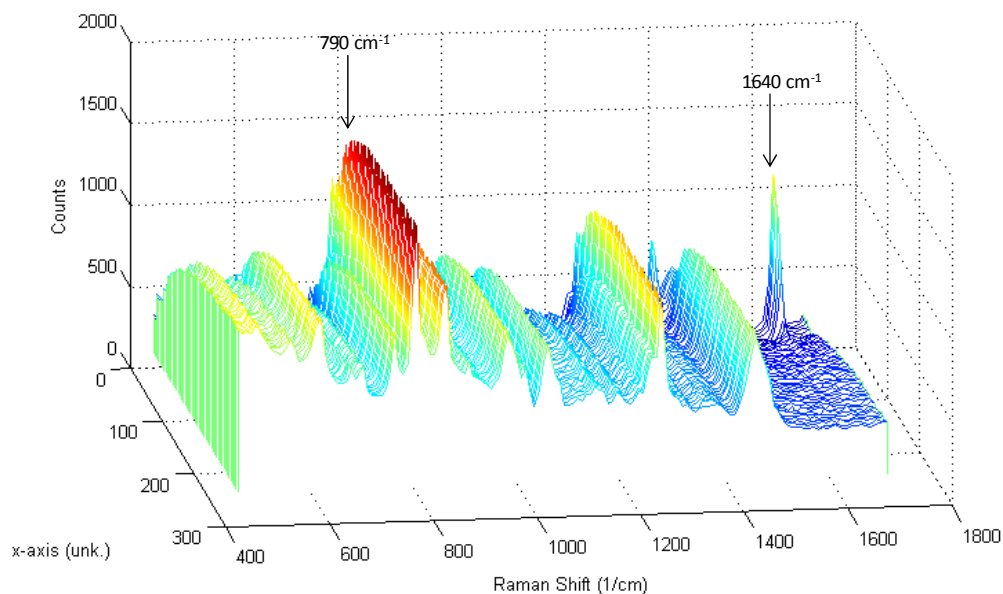


Figure C3: Real-time Raman waterfall plot of METHHB with 0.17 wt% DMPA. Free-radical only photopolymerization with an effective irradiance of 100 mW/cm<sup>2</sup> at 70°C.

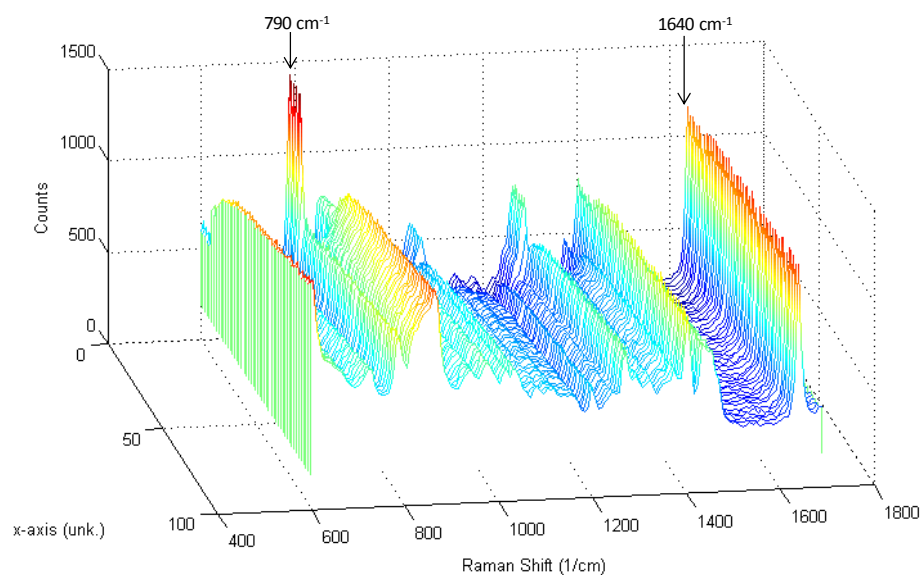


Figure C4: Real-time Raman waterfall plot of METHHB with 0.5 wt% DAI. Cationic only photopolymerization with an effective irradiance of 100 mW/cm<sup>2</sup> at 70°C.



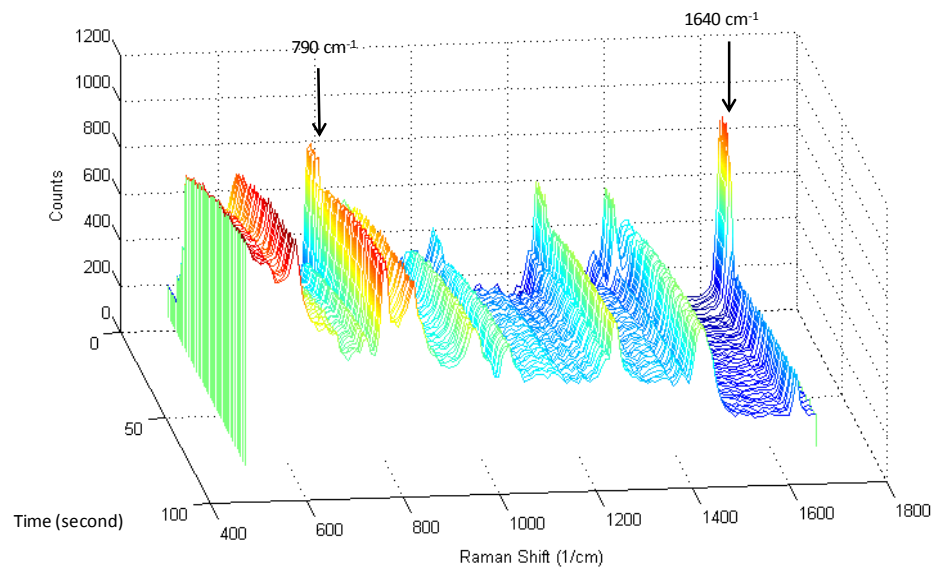


Figure C5: Real-time Raman waterfall plot of METHHB with 0.5 wt% DAI and 0.17 wt% DMPA. Free-radical and cationic photopolymerization with an effective irradiance of 100 mW/cm<sup>2</sup> at 30°C.

## APPENDIX D

### SHRINKAGE STRESS ANALYSIS

Several analytical approaches are available for measuring polymerization shrinkage. Some methods are based on volume change such as fluid dilatometer<sup>1</sup> and gas pycnometer;<sup>2</sup> others measure shrinkage stress by dividing the measured tensile force by cross-sectional area of the sample, such as using a tensometer<sup>3</sup> and polymerization stress tester designed to measure polymerization stress and shrinkage. In a fluid dilatometer, an uncured sample is immersed in an immiscible fluid, such as mercury or water, which extends to a graduated capillary tube that is attached to a bulb. The change in volume of the sample is noted by measuring the change in height of the fluid in the capillary tube.<sup>4</sup> Similarly, a pycnometer measures the change in volume of a sample during cure. The instrument has two connected chambers of known volume, with the sample placed in one of the chambers. When the sample is cured, gas is allowed to enter into the sample chamber from the other chamber. The sample volume is calculated via Boyle's law from the change in pressure of the gas from the other chamber before and after curing of the sample.

The tensometer is based on a basic engineering beam theory that a tensile force generated by the bonded shrinkage sample causes a cantilever beam to deflect. The deflection of the beam is measured with a linear variable differential transformer. The tensile force is calculated based on a calibration constant for the beam that is dependent on the distance between the clamped end of the cantilever beam and the sample position along the beam. Shrinkage stress is obtained by dividing the measured tensile force by the cross-sectional area of the sample.<sup>5</sup>

Polymerization shrinkage stress tester (Proto-tech, Portland, OR) is based on cylindrical testing geometry that uses a precision positioning stage driven by a stepping motor (see Figure 1.3). The advantage it has over other methods is that sample preparations for each specimen are quick and easy to perform. A 200N load cell senses the polymerization stress, and the level of compliance correction can be adjusted up to 100% compensation for compliance of the load cell. The up and down motion of the stage is controlled through a command module. The polymerization stress or the polymerization shrinkage of the composite can be measured with the apparatus, depending on the testing mode selected. The testing fixtures allow for light curing to be directed to both the top and bottom sides of the specimen.<sup>6</sup> This method could be paired with Raman spectroscopy to obtain real-time kinetics together with polymerization shrinkage.

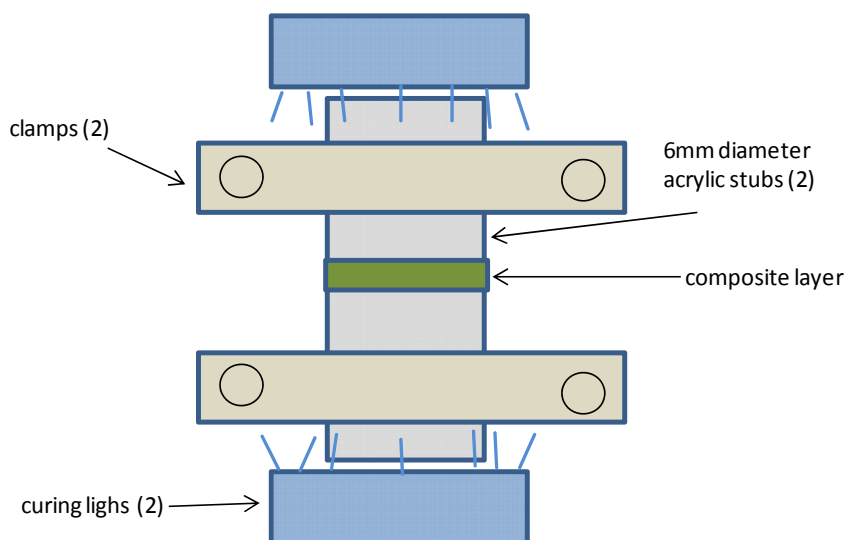


Figure D1: Schematic of polymerization stress tester, used to monitor polymerization shrinkage.

Notes

1. Ramsteiner, F. Fluid Dilatometer to Measure the Volume Change of Polymeric Materials During Tensile Tests. *Polymer Testing*. 1996;15:401-405.
2. Tamari S. Optimum Design of The Constant-Volume Gas Pycnometer for Determining the Volume of Solid Particles. *Measurement science technology*. 2004;15:549-558.
3. Lu, H.; Stansbury, J.W.; Bowman ,C.N. Impact of Curing Protocol on Conversion and Shrinkage Stress. *Journal of Dental Research*. 2005;84:822-826.
4. Parlevliet, P.; Barsee, H.E.N.; Beukers, A. Shrinkage Determination of a Reactive Polymer with Volumetric Dilatometry. *Polymer Testing*. 2010;29:433-439.
5. Lu,H.; Stansbury, J.W.; Eichmiller, F.C. Probing the Origins and Control of Shrinkage Stress in Dental Resin-Composites: I. Shrinkage Stress Characterization Technique. *Journal of materials science.Materials in medicine*. 2004;15:1097-1103.
6. Condon, J.R. Polymerization Stress of Twelve Commercial Composites. <http://oralwear.net/>. (Accessed, February, 1st 2012).

## REFERENCES

- Abdul-Rasoul, F.A.M. Photochemical and Thermal Cationic Polymerizations Promoted by Free Radical Initiators. *Polymer*. 1978;19:1219.
- Andrzejewska, E. Photopolymerization Kinetics of Multifunctional Monomers. *Progress in polymer science*. 2001;26:605-665.
- Barabas, I.; Todorut, I. Predicting the Temperature Dependent Viscosity of Biodiesel-Diesel-Bioethanol Blends. *Energy Fuels*. 2011;25:5767-5774.
- Bates, F.S. Polymer-Polymer Phase Behavior. *Science*. 1991;251:898-905.
- Bednarek, M.; Kubisa, P.; Penczek, S. Coexistence of Activated Monomer and Active Chain End Mechanisms in Cationic Copolymerization of Tetrahydrofuran with Ethylene oxide. *Macromolecules*. 1999;32:5257-5263.
- Benson, S.W.; North, A.M. The Kinetics of Free Radical Polymerization under Conditions of Diffusion-Controlled Termination. *Journal American Chemical Society*. 1962;84:935-940.
- Beuermann, S.; Buback, M.; Davis, T.P, Gilbert, R.G.; Hutchinson, R.A.; Olaj, O.F.; Russel, G.T.; Schweer, J.; Alex, M.H. Critically Evaluated Rate Coefficients for Free-Radical Polymerization, 2. Propagation Rate Coefficients for Methyl Methacrylate. *Macromolecular Chemistry and Physics*. 1997;198:1545-1560.
- Biedron, T.; Szymanski, R.; Kubisa, P.; Penczek, S. Kinetics of Polymerization by Activated Monomer Mechanism. *Makromolekulare Chemie-Macromolecular Symposia*. 1990;32:155-168.
- Braslaw, R. Handbook of Radical Polymerization. Edited by Krzysztof Matyjaszewski, (Carnegie Mellon University) and Thomas P. Davis, (University of New South Wales). John Wiley & Sons, Inc.: Hoboken. *Journal of American Chemical Society*. 2003;125:3399-3400.
- Burdick, J.; Lovestead, T.M.; Anseth, K.S. Kinetic Chain Lengths in Highly Cross-linked Networks Formed by the Photoinitiated Polymerization of Divinyl Monomers: A Gel Permeation Chromatography Investigation. *Biomacromolecules*. 2003;4:149.
- Cai, Y.; Jessop J.L.P. Effect of Water Concentration on Photopolymerized Acrylate/Epoxy Hybrid Polymer Coatings as Demonstrated by Raman Spectroscopy. *Polymer*. 2009;50:5406.
- Cai, Y.; Jessop J.L.P. Photopolymerization, Free Radical. In *Encyclopedia of Polymer Science and Technology*. 2003:807-837.
- Cai, Y. Effect of Water Concentration on Photopolymerized Acrylate/Epoxy Hybrid Polymer Coatings as Demonstrated by Raman Spectroscopy. *Polymer*. 2009;50:5406.

- Cai, Y.; Jessop, J.L.P. Decreased Oxygen Inhibition in Photopolymerized Acrylate/Epoxy Hybrid Polymer Coatings as Demonstrated by Raman Spectroscopy. *Polymer*. 2006;47:6560-6566.
- Chien, J.C.W.; Cheun, Y.; Lillya, C.P. Cationic Polymerizations of Dioxepane and Its 2-Alkyl Derivatives. *Macromolecules*. 1988;21:870-875.
- Cho, J. UV-initiated Free-radical and Cationic Photopolymerizations of Acrylate/Epoxy and Acrylate/Vinyl Ether Hybrid Systems with and without Photosensitizer. *J Applied Polymer Science*. 2004;93:1473.
- Chong, J.S. Oxygen Consumption During Induction Period of Photopolymerizing System. *Journal of Applied Polymer Science*. 1969;13:241.
- Condon, J.R. Polymerization Stress of Twelve Commercial Composites. <http://oralwear.net/>. (Accessed February, 1, 2012).
- Crivello J. Design and Synthesis of Highly Reactive Photopolymerizable Epoxy Monomers. *Journal of Polymer Science.Part A, Polymer Chemistry*. 2001;39:2385-2395.
- Crivello, J. Synergistic Effects in Hybrid Free Radical/Cationic Photopolymerizations. *Journal of Polymer Science. Part A, Polymer Chemistry*. 2007;45:3759.
- Crivello, J.V. Photoinitiated Cationic Photopolymerization. *Annual review of materials science*. 1983;13:173-190.
- Davidson, C.L.; Feilzer, A.J. Polymerization Shrinkage and Polymerization Shrinkage Stress in Polymer-Based Restoratives. *Journal Dental Research*. 1997;25:435-440.
- Decker C. UV-radiation curing of acrylate/epoxy systems. *Polymer*. 2001;42:5531-5541.
- Decker, C. Photoinitiated Crosslinking Polymerization. *Progress in Polymer Science*. 1996;21:593-650.
- Decker, C.; Decker, D.; Morel, F. Light Intensity and Temperature Effect in Photoinitiated Polymerization. *American Chemical Society Symposium Series*. 1997:63-63
- Decker, C.; Viet, T.N.T.; This, H.P. Photoinitiated Cationic Polymerization of Epoxides. *Polymer International*. 2001;50:986-997.
- Dewaele, M. Volume Contraction in Photocured Dental Resins: The Shrinkage-Conversion Relationship Revisited. *Dental Materials*. 2006;22:359-365.
- Doorn, S. Raman Spectroscopy and Imaging of Ultralong Carbon Nanotubes. *The journal of physical chemistry. B*. 2005;109:3751-3758.

Dreyfuss, P.; Dreyfuss, M.P. *Chapter 4 Polymerization of Cyclic Ethers and Sulphides. /: . Comprehensive Chemical Kinetics*. Elsevier:259-330.

Duan, J.; Kim, C.; Jiang, P. On-line Monitoring of Cycloaliphatic Epoxy/Acrylate Interpenetrating Polymer Networks Formation and Characterization of their Mechanical Properties. *Journal of Polymer Research*. 2009;16:45-54.

Foreman, J. Dynamic Mechanical Analysis of Polymers. *American Laboratory*. 1997;29:21-24.

Fouassier, J.P. Photopolymerization Reactions Under Visible Lights: Principle, Mechanisms and Examples of Applications. *Progress in organic coatings*. 2003;47:16-36.

Gary, C. RadTech Annual Review, 2005-2006. [http://www.radtech.org/corporate/press2006/RT\\_Annual\\_Report\\_05-06.pdf](http://www.radtech.org/corporate/press2006/RT_Annual_Report_05-06.pdf). (Accessed June, 12th, 2010).

Geiser, V. Conversion and Shrinkage Analysis of Acrylated Hyperbranched Polymer Nanocomposites. *Journal of applied polymer science*. 2009;114:1954-1963.

Ghosh, N.; Palmese G. Electron-Beam Curing of Epoxy Resins: Effect of Alcohols on Cationic Polymerization. *Bulletine of Material Science*. 2005;28:603-607.

Gleeson, M. Modeling the Photochemical Effects Present during Holographic Grating Formation in Photopolymer Materials. *Journal of Applied Physics*. 2007;102(2); 023108-1-023108-8

Gudzera, S.S. Microphase Structure of Photopolymerizable Hybrid Adhesives Based on Urethane-Acrylates, Alkyd-Epoxy Resins and Polyisocyanates. *Polymer Science Series A*. 1991;33:2288-2295.

He, J.; Mendoza, V.S. Synthesis and Study of a Novel Hybrid UV Photoinitiator: p-benzoyldiphenyliodonium hexafluorophosphate ( $\text{PhCOPhI}^+ \text{PhPF}_6^-$ ). *Journal of polymer science.Part A, Polymer chemistry*. 1996;34:2809-2816.

He, Y. Photopolymerization Kinetics of Cycloaliphatic Epoxide-Acrylate Hybrid Monomer. *Polymer International*. 2007;56:1292-1297.

He, Y.; Xiao, M.; Wu, F.; Nie, Jun. Photopolymerization Kinetics of Cycloaliphatic Epoxide-Acrylate Hybrid Monomer. *Polymer International*. 2007;56:1292-1297.

Hofer, M.; Moszner, N.; Liska, R. Oxygen Scavengers and Sensitizers for Reduced Oxygen Inhibition in Radical Photopolymerization. *Journal Polymer Science Part A*. 2008;46:6916-6927.

Jančovičová, V.; Brezová, V.; Ciganek, M.; Cibulková, Z. Photolysis of Diaryliodonium Salts (UV/Vis, EPR and GC/MS investigations). *Journal Photochemistry and Photobiology A*. 2000;136:195-202.

Johnson, A.; Lewis, I.; Edwards, H. Applications of Raman-Spectroscopy to The Study of Polymers and Polymerization Process. *Journal of Raman Spectroscopy*. 1993;24:475-483.

Johnson, C.K. Picosecond Timescale Raman Processes and Spectroscopy. *Pure and applied chemistry*. 1984;57:195-200.

Ju-Young, K.; Yong-Seok, C.; Kyung-DO, S. Microphase-Separated Structure of Telechelic Urethane Acrylate Anionomers and Their Network in Various Solvents. *Journal of polymer science.Part B, Polymer physics*. 2000;38:2081-2095.

Keogh, T.P. Vacuum or Suction Adhesion. <http://www.blogdental.es/Keogh/?p=131>. (Accessed, March 8th, 2012).

Khandare, P.M. Measurement of the Glass Transition Temperature of Mesophase Pitches using a Thermomechanical Device. *Carbon*. 1996;34:663-669.

Koleske, J.V. Cationic Photoinitiators and Initiation Mechanism. *In Radiation Curing of Coatings, ASTM International. Bridgeport, NJ*. 2002:55-67.

Koleske, J.V. Cationic Photoinitiators and Initiation Mechanism. In: *Radiation Curing of Coatings*. Bridgeport, NJ: ASTM International, 2002:55-66.

Krzysztof, L. Spectroscopic and Photopolymerization Studies of Benzyl Methacrylate/Poly(Benzyl Methacrylate) Two-Component System. *Journal of polymer science.Part B, Polymer physics*. 2010;48:1336-1348.

Lee, T.Y.; Guymon, C.A.; Jonsson, S.E.; Hoyle, C.E. The Effect of Monomer Structure on Oxygen Inhibition of (meth)acrylates Photopolymerization. *Polymer*. 2004;45:6155-6162.

Lee, T.Y.; Roper, T.M.; Jonsson, S.E.; Guymon, C.A.; Hoyle, C.E. Influence of Hydrogen Bonding on Photopolymerization Rate of Hydroxyalkyl Acrylates. *Macromolecules*. 2004;37:3659-3665.

Leung, D.; Bowman, C.N. Reducing Shrinkage Stress of Dimethacrylate Networks by Reversible Addition-Fragmentation Chain Transfer. *Macromolecular chemistry and Physics*. 2012;213:198-204.

Lin, Y.; Stansbury, J.W. Kinetics Studies of Hybrid Structure Formation by Controlled Photopolymerization. *Polymer*. 2003;44:4781-4789.



- Lin, Y.; Stansbury, J.W. The Impact of Water on Photopolymerization Kinetics of Methacrylate/vinyl Ether Hybrid Systems. *Polymer Advanced Technologies*. 2005;16:195-199.
- Lu, H.; Stansbury, J.W.; Bowman, C.N. Impact of Curing Protocol on Conversion and Shrinkage Stress. *Journal of Dental Research*. 2005;84:822-82
- Lu, H.; Stansbury, J.W.; Eichmiller, F.C. Probing the Origins and Control of Shrinkage Stress in Dental Resin-Composites: I. Shrinkage Stress Characterization Technique. *Journal of materials science. Materials in medicine*. 2004;15:1097-1103.
- Maddams W, Gerrard D. Polymer Characterization by Raman-Spectroscopy. *Applied spectroscopy reviews*. 1986;22:251-334.
- Maslyuk, A. F.; Khranovskii, V.A.; Lipatov, Y.S.; Grishchenko, V. K. IR-Spectroscopic Study of the Process of Photopolymerization of Polyvinyl Compounds. *Polymer science*. 1984;26:1479-1483.
- Mathew, Viju.; Sinturel, C. Epoxy Resin/Liquid Natural Rubber System: Secondary Phase Separation and its Impact on Mechanical Properties. *Journal of Material Science*. 2010;45:1769-1781.
- Menard K. Dynamic Mechanical Analysis: A Practical Introduction. *Second Edition. CRC Press Boca Raton London New York Washington, D.C.* 2008.
- Mitlin, V.S.; Manevich, L.I. Kinetically Stable Structures in the Nonlinear Theory of Spinodal Decomposition. *Journal of polymer science. Part B, Polymer physics*. 1990;28:1-16.
- Monroe, B. Photoinitiators for Free-Radical-Initiated Photoimaging Systems. *Chemical Review American Chemical Society*. 1993;93:435-448.
- Montserrat, S. Measuring the Glass Transition of Thermosets by Alternating Differential Scanning Calorimetry. *Journal of Thermal Analysis and Calorimetry*. 2000;59:289-303.
- Moussa, K.; Decker, C. Light-Induced Polymerization of New Highly Reactive Acrylic Monomers. *Journal of Polymer Science Part A: Polymer Chemistry*. 1993;31:2197-2203
- Nelson, E.W.; Scranton, A.B. In Situ Raman Spectroscopy for Cure Monitoring of Cationic Photopolymerizations of Divinyl Ethers. *Journal of Raman Spectroscopy*. 1996;27:137-137.
- O'Brien, K.A.; Bowman, C.N. Modeling the Effect of Oxygen on Photopolymerization Kinetics. *Macromolecular Theory and Simulations*. 2006;15:176-182.
- Odian, G.G. *Principles of Polymerization / George Odian*. (Fourth Edition edition). New York: Wiley, 2004. Page 204-207, 271

- Oxman, J.D.; Jacobs, D.W.; Trom, M.C.; Sipani, V.; Ficek, B.; Scranton, A.B. Evaluation of Initiator Systems for Controlled and Sequentially Curable Free-radical/Cationic Hybrid Photopolymerizations. *Journal of Polymer Science Part A: Polymer Chemistry*. 2005;43:1747-1756.
- Palmese, G.R.; Ghosh, N.N.; McKnight, S.H. Investigation of Factors Influencing the Cationic Polymerization of Epoxy Resins. *International SAMPE Symposium and Exhibition*. 2000;45.
- Parlevliet, P.; Barsee, H.E.N.; Beukers, A. Shrinkage Determination of a Reactive Polymer with Volumetric Dilatometry. *Polymer Testing*. 2010;29:433-439.
- Penczek, S.; Kubisa, P.; Szymanski, R. Activated Monomer Propagation in Cationic Polymerizations. *Makromolekulare Chemie-Macromolecular Symposia*. 1986;3:203-220.
- Peter, D.G. Structured Illumination as a Processing Method for Controlling Photopolymerized Coating Characteristics. *PhD Thesis, University of Iowa*, 2007.
- Rajaraman, S.K.; Mowers, W.A.; Crivello, J.V. Interaction of Epoxy and Vinyl Ethers during Photoinitiated Cationic Polymerization. *J Polymer Science Part A*. 1999;37:4007-4018.
- Ramsteiner, F. Fluid Dilatometer to Measure the Volume Change of Polymeric Materials During Tensile Tests. *Polymer Testing*. 1996;15:401-405.
- Rhodes K. Adhesives Deliver Low Shrink, Low Stress Bonds and Fast UV Cure. *Proceedings of SPIE--the international society for optical engineering*. 2001;4253:92-107.
- Russell, B.; Chartoff, R.; The Influence of Cure Conditions on the Morphology and Phase Distribution in a Rubber-Modified Epoxy Resin using Scanning Electron Microscopy and Atomic Force Microscopy. *Polymer*. 2005;46:785-798.
- Sangermano, M.; Carbonaro, W.; Malucelli, G.; Priola, A. UV-Cured Interpenetrating Acrylic-Epoxy Polymer Networks: Preparation and Characterization. *Macromolecular Materials and Engineering*. 2008;293:515-520.
- Sangermano, M.; Carbonaro, W.; Malucelli, G.; Priola, A. Bicyclo-Orthoester as a Low-Shrinkage Additive in Cationic UV curing. *Polymer International*. 2007;56:1224-1229.
- Sartomer Application Bulletin. Shrinkage of UV Monomers. <http://www.sartomer.com/TechLit/4029.pdf>. 2011 (Accessed, Feb, 1st 2012).
- Sartomer Application Bulletin. UV Curable Monomers Properties: Shrinkage and Glass Transition. <http://www.sartomer.com/TechLit/4039.pdf>. 2011. (Accessed, Feb, 1st 2012).
- Schikowsky, V.; Timpe, H. Investigation on Photolysis of Diaryliodonium Salts. *Journal für Praktische Chemie*. 1989;331:447-460.

Sims, D. Polymerisation of tetrahydrofuran (part II). *Die Makromolekulare Chemie*. 1966;98:235-244.

Sipani, V.; Scranton, A.B. Photopolymerization, Cationic. In *Encyclopedia of Polymer Science and Technology*, 2003:784-807.

Sipani, V.; Kirsh, A.; Scranton, A.B. Dark cure Studies of Cationic Photopolymerizations of Epoxides: Characterization of Kinetic Rate Constants at High Conversions. *Journal of polymer science. Part A, Polymer chemistry*. 2004;42:4409-4416.

Sipani, V.; Scranton, A.B. Dark-Cure Studies of Cationic Photopolymerizations of Epoxides: Characterization of the Active Center Lifetime and Kinetic Rate Constants. *Journal of polymer science. Part A, Polymer chemistry*. 2003;41:2064-2072

Strehmel, V.; Strehmel, B. Photoinduced Crosslinking of a Liquid-Crystalline Monomer in Thin Films. *Thin Solid Films*. 1996;284:317.

Studer, K.; Decker, C.; Schwalm, R. Overcoming Oxygen Inhibition in UV-curing of Acrylate Coatings by Carbon dioxide Inerting: Part II. *Progress in Organic Coatings*. 2003;48:101-111.

Tamari S. Optimum Design of The Constant-Volume Gas Pycnometer for Determining the Volume of Solid Particles. *Measurement science technology*. 2004;15:549-558.

Tanaka, H. Coarsening Mechanisms of Droplet Spinodal Decomposition in Binary Fluid Mixtures. *Journal of Chemical Physics*. 1996;105:10099-10099.

Tryson, C.R.; Shultz A.R. A Calorimetric Study of Acrylate Photopolymerization. *Journal of Polymer Science: Polymer Physics Edition*. 1979;17:2059-2075.

Vaidyanathan, J.; Vaidyanathan, T.K. Dynamic Mechanical Analysis of Heat, Microwave and Visible Light Cure Denture Base Resins. *Journal of Materials Science, Materials in Medicine*. 1995;6:670-674.

Wei, H.; Li, Q.; Ojelade, M.; Madbouly, S.; Otaigbe, J.U.; Hoyle, C.E. Thiol-Ene Free-Radical and Vinyl Ether Cationic Hybrid Photopolymerization. *Macromolecules*. 2007;40:8788-8793.

Wei, H.; Senyurt, A.F.; Jonsson, S.E.; Hoyle, C.E. Photopolymerization of Ternary Thiol-Ene/Acrylate Systems: Film and Network Properties. *Journal of polymer science. Part A, Polymer chemistry*. 2007;45:822-829.

Wight, F. Oxygen Inhibition of Acrylic Photopolymerization. *Journal of Polymer Science Polymer Letter Edition* 1978;16:121-127.

Williams, J.B.; Takeshi, E. Radical Ring-Opening Polymerization and Copolymerization with Expansion in Volume. *Journal of Polymer Science, Polymer Symposia*. 1978;64:17-26.

Yamada, B.; Kobatake,S.; Aoki,S. Rate Constants for Elementary Reactions of the Radical Polymerization of Methyl 2-(Benzyloxymethyl)Acrylate as Polymerizable Acrylate Bearing Large Substitutents. *Macromolecular Chemistry and Physics*. 1994;195:933-942.

Yanada, B.; Kobatake,S.; Aoki,S. Rate Constants for Elementary Reactions of the Radical Polymerization of Methyl 2-(Benzyloxymethyl)Acrylate as Polymerizable Acrylate Bearing Large Substitutents. *Macromolecular Chemistry and Physics*. 1994;195:933-942.

Zak, G.; Sela, M.N.; Yevko, V.; Park, C.B.; Benhabib, B. Layered-Manufacturing of Fiber-Reinforced Composites. *Journal of Manufacturing Science and Engineering*. 1999;121:448-456.

Zhang,Y.; Yang, X.; Zhaoa, X.; Huang, A. Synthesis and Properties of Optically Clear Silicone Resin/Epoxy Resin Hybrids. *Polymer International*. 2012;61:294-300